

MODELING THE DYNAMICS OF ENTEROVIRUS-71 IN TAIWAN: An application of the TSIR model

Emily Tseng

Department of Ecology and Evolutionary Biology

Princeton University

Professor Bryan Grenfell

April 28, 2014

Acknowledgements

First and foremost, I am indebted to my adviser, **Professor Bryan Grenfell**, who has been not just a critical source of guidance and encouragement throughout this thesis project but also an academic inspiration throughout my time at Princeton. As a wayward sophomore I had a variety of interests but no real focus—one meeting with Professor Grenfell gave me a department to join, a whole new area of research in which to immerse myself, a slate of courses to take and the promise that I would learn something intellectually engaging, truly useful and, honestly, fun. One zombie project, two JPs and one thesis later, I can say that promise has held true.

Perhaps the best part of my education has been the privilege of experiencing the collegiality, dedicated intelligence and good vibes of everyone in the Department of Ecology & Evolutionary Biology. **Dr. Tiffany Bogich** initially presented the idea for this project and has also been critical to its success. Thanks to Dr. Bogich and also to **Dr. Quentin Caudron, Dr. Jessica Metcalf, Dr. Jon Zelner, Ruthie Birger** and **Saki Takahashi**, for their kindness, time and patience in teaching me how to model.

In addition to my academic mentors and advisers, I must thank the **Center for Health & Wellbeing (Global Health Program)** for its exceptional generosity in funding my summer adventures in Vietnam at the **Oxford University Clinical Research Unit**.

Special thanks to **Devika Balachandran** and **Tim Trieu**, for steadfast, tried-and-true friendship; for listening to me babble about susceptible reconstruction and helping me battle my code; and for only teasing me a little bit when I muddled the basic principles of linear regression.

Thanks to Phil, Melissa and everyone else at MSF, for inspiring in me a passion for global and public health. To my family, for critical help in reading Chinese websites and for all the gentle thesis reminders over the last eight months. To Nikki, for stunningly effective pep talks, and to Sharon, Nick and the dinosaur of Guyot Hall, for lowkey-highkey support through this last sleepless push.

Thanks to my friends, for suffusing these four years with the opposite of loneliness. And thanks, finally, to the Terrace F. Club, for making my time here so weird, wonderful and bright. See Fig. A4.

Abstract

Background: Human Enterovirus-71 (EV-71) is an emerging pathogen that has become a novel target for disease surveillance and control efforts in the Asia-Pacific region. EV-71 and the group A coxsackieviruses are the major causative agents of Hand, Foot & Mouth Disease (HFMD), normally a self-limiting childhood infection transmitted via the fecal-oral route that causes a rash of vesicular lesions on the hands, feet and oral mucosa. The majority of individuals infected with HFMD require little to no medical attention; in some cases, however, enterovirus infection leads to severe neurologic complications like encephalitis, meningitis, myocarditis and acute paralysis.

Research goals: EV-71 poses a disease modeling challenge, as existing data captures only severe cases and not the true burden of infection. This thesis aims to mathematically derive the true burden of EV-71 infection in Taiwan, to elucidate key epidemiological parameters from available data using a stochastic, discrete-time modeling approach, and to use those parameters to model the potential impact of vaccination.

Methods: Data were sourced from publicly available databases maintained by the Taiwan Center for Disease Control. The Time series-Susceptible-Infected-Recovered (TSIR) model was used for parameter inference and simulation.

Results: Key modeling parameters were elucidated from the dataset, including 53 weekly transmission parameters, an overall contact mixing parameter and a reconstructed susceptibles class. The true burden of infection was estimated to be 1492 times the reported number of cases. Simulations forecasting vaccination identified a critical population coverage level at 99.95%.

Conclusion: In the case of severe enterovirus infection, the TSIR modeling approach provides a useful tool for the extrapolation of epidemiological parameters from a limited dataset. If proper forecasting is to be done for EV-71, however, more work is needed to clarify disease characteristics and allow for more complex modeling.

Table of Contents

Acknowledgements	i
Abstract	ii
List of figures and tables.....	iv
Introduction.....	1
1. Biology of enterovirus-71	2
1.1. Adaptation and evolution.....	3
2. Global epidemiological history	5
2.1. EV-71 and HFMD.....	7
2.2. The 1998 outbreak in Taiwan	7
2.3. Recent activity	9
3. Questions in pathogenicity.....	9
4. Coxsackievirus-16	10
5. Research goals	11
Methods	12
1. Data	12
2. Modeling.....	13
2.1. The TSIR Model	14
2.2. State variable reconstruction & parameter inference	15
2.3. Simulation	17
Results	18
1. Descriptive analysis	18
1.1. Age distribution.....	19
1.2. Seasonality	20
2. Parameter derivation.....	22
2.1. Underreporting.....	24
2.2. Susceptible reconstruction.....	24
2.3. Model fit	26
3. Simulation	27
4. Vaccination	29
Discussion.....	31
1. Key results.....	31
2. Challenges.....	34
3. Future directions	36
Appendix	38
References	42

List of figures and tables

Figure 1	Capsid structure of EV-71 (from Plevka 2012)	3
Figure 2	Reported EV-71 epidemics, 1970-2000 (from Bible 2007)	6
Figure 3	Cases of HFMD/herpangina infection reported in Taiwan, March-December 1998 (from Ho 2000)	8
Figure 4	Sample SIR Model Schematic (from Tseng 2013)	14
Figure 5	Reported weekly incidence of severe enterovirus infection in Taiwan, 1999-2013	18
Figure 6	Cumulative proportions of reported infection at each age	19
Figure 7	Age distribution of reported cases per year	20
Figure 8	Weekly time series of cases, by year	21
Figure 9	Wavelet analysis of epidemic periodicity	22
Figure 10	Average weekly course of transmission and infection	23
Figure 11	Reconstructed susceptibles and reported infecteds	25
Figure 12	Model fit	26
Figure 13	Simulated infecteds course using national birth rates from 1999-2013	27
Figure 14	Effect of varying contact rates on simulated infecteds courses	28
Figure 15	Time series of simulated infecteds courses at increasing levels of vaccination coverage	29
Figure 16	Effect of increasing vaccination coverage on the number of infecteds at endpoint	30
Figure A1	Regression of cumulative cases against cumulative births	Appendix
Figure A2	Reporting rates over time	Appendix
Figure A3	Derivation of mean susceptibles	Appendix
Table 1	Key parameters	22
Table 2	Transmission parameters (β)	Appendix

Introduction

Human Enterovirus-71 (EV-71) is an emerging pathogen that has become a novel target for disease control efforts in the Asia-Pacific region. EV-71 and the group A coxsackieviruses are the major causative agents of Hand, Foot & Mouth Disease (HFMD), normally a self-limiting childhood infection transmitted via the fecal-oral route that causes a rash of vesicular lesions on the hands, feet and oral mucosa [1]. The majority of individuals with HFMD require little to no medical attention; in some cases, however, enterovirus infection leads to severe neurologic complications like encephalitis, meningitis, myocarditis and acute paralysis. These severe sequelae have been known to result in rapid clinical deterioration and death.

In the Southeast Asian island nation of Taiwan in 1998, a large-scale outbreak of enterovirus infection saw an estimated 1.5 million cases of HFMD/herpangina [2].¹ 405 of those cases resulted in severe sequelae, of which 78 infections resulted in death. EV-71 was isolated from 92 percent of the patients who died in the Taiwan epidemic, and is acknowledged to be the most frequently detected viral agent in HFMD patients with severe neurologic complications [4],[5]. Since its identification in California in 1974, it has also been implicated as the pathogen responsible for outbreaks in Hungary, Australia, Hong Kong, Japan, Singapore, Malaysia and mainland China [6]–[12].

EV-71 has emerged as a clinically relevant pathogen with a global reach—yet effective treatments and vaccines have yet to be made available [5], [13]. Overshadowed perhaps by its relative the poliovirus, which has a much longer history and a higher profile as a public threat, the pathogen has only in the last decade become a target for

¹ Herpangina, clinically defined as oral ulcerations located on the tonsils, soft palate, buccal mucosa or uvula, is a hallmark of coxsackievirus infection. Cases of HFMD are known to present in combination with herpangina [33].

dedicated vaccine development. The first candidate EV-71 vaccines are currently undergoing safety trials in Taiwan, China and Singapore [14].

The relatively short history of the virus presents a novel area of inquiry. What are the epidemiological parameters of the virus's behavior? Can current mathematical models capture its epidemiology? What are the control possibilities afforded by the development of an EV-71 vaccine? Growing out of work completed for my junior paper [15], this thesis seeks to model the effect successful vaccination could have on the incidence of enterovirus infection in Taiwan.

This introduction will discuss: 1) biological features of EV-71, 2) the history of the virus, 3) issues in pathogenicity and clinical presentations of disease, 4) related viruses implicated alongside EV-71 in outbreaks and 5) the goals of this thesis.

1. BIOLOGY AND EVOLUTION OF ENTEROVIRUS-71

Structurally, EV-71 is a non-enveloped, positive-stranded RNA virus in the family *Picornaviridae* with a genome approximately 7,500 bases long [16]. It consists of four capsid proteins, VP1 to VP4, and seven nonstructural proteins, termed 2A, 2B, 2C, 3A, 3B, 3C and 3D. As seen in other enteroviruses like the poliovirus, the capsid proteins of EV-71 are assembled in a symmetrical icosahedral lattice as pentameric subunits (Fig. 1). The capsid consists of 60 such subunits, each containing structural proteins VP1-VP4.

Capsid proteins VP1, VP2 and VP3 are known to recognize receptors on the surface of specific host cells and to be antigenic [17]. Of these, the VP1 site is considered most relevant for neutralizing immunity, as the structural loops of the VP1 region exposed on the surface of the virus are the region most commonly targeted by host antibodies [18].

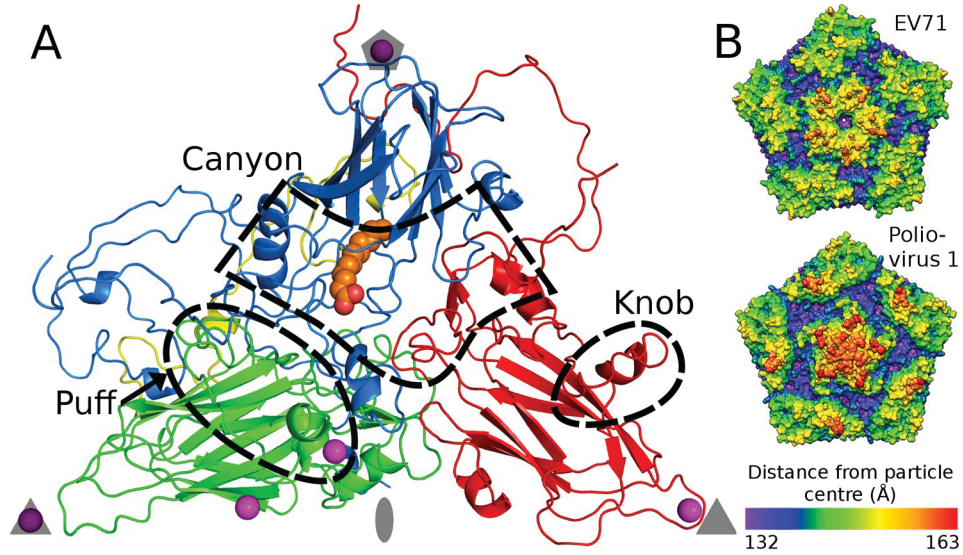


FIGURE 1: CAPSID STRUCTURE OF EV-71 (FROM PLEVKA 2012). A) Diagram of an icosahedral unit. VP1 is shown in blue, VP2 in green, VP3 in red and VP4 in yellow. Prominent surface features are indicated by dashed lines. B) Diagram of EV-71 and Poliovirus 1 demonstrating the similarity between the two.

Using that region as a reference point, Brown et al. in 1999 identified three genogroups of EV-71, termed A, B and C [19]. The prototype strain, named BrCr, is the only known member of genogroup A. Subgenogroups B1-B5 and C1-C5 are the most common strains circulating in human populations. Within a genogroup, genomic variation between subgenogroups does not exceed 10%.

1.1 Adaptation and evolution²

Evolutionary studies of EV-71 show that the virus emerged in the mid-1900s but has been more rapidly evolving in the last thirty years, with an estimated variation rate of 1.35×10^{-2} substitutions per nucleotide [16]. This mutation rate is similar to that observed for the poliovirus. Much of this increase in variation is attributed to the generation of new strains brought about by genogroup cocirculation in human

² This section grows out of work I conducted for my fall JP.

populations. In 2005, a study in the Yamagata Prefecture of Japan found four different subgenogroups of EV-71 circulating concurrently, with a C4 to novel B5 subgenogroup overturn observed within a matter of months [20], [21].

Most evolutionary studies have focused on the exposed VP1 region, which is thought to be the site of the genome most susceptible to selective pressure. Chen et al. in 2010 found evidence of positive selection at site 145 of the VP1 region, among evidence of negative or purifying selection throughout the rest of the coding region [17]. Tee et al. in 2007 found evidence of rapid amino acid “toggling” in the VP1 coding regions of core trunk branches of a reconstructed EV-71 phylogeny [16]. It was hypothesized that toggling, a phenomenon in which the amino acid at a certain position mutates and persists as a different amino acid before reverting to its original residue, might indicate adaptive mutations, perhaps in the context of host immune response. Tee et al. also found that their reconstructed EV-71 lineage resembled the ladder lineage of influenza, which is known to evolve to evade host defenses each season. Taken together, these results evidence the possibility that EV-71 evolution is driven by immune escape.

In contrast, McWilliam Leitch et al. in 2012 put forth a different scheme of EV-71 evolution in which recombination did not rely on adaptive swaps at immunologically relevant sites like the VP1 region but rather on independent, non-systemic swaps in the non-structural coding sequences [22]. This alternate scheme, the group noted, was observed in enteroviruses B. This pattern of mutation was to be considered decoupled from patterns of genetic selection at specific capsid regions. The group further argued that the evidence for positive selection in the EV-71 genome was limited at best. If adaptive evolution in response to immune selection was driving mutation, the range of existing viral strains should have exhibited antigenic diversity consistent with exposure to different host populations. But cross-neutralization experiments have not yielded robust evidence for subgenogroup-specific antibodies, the group claimed.

The question of which scheme of evolution drives and governs the EV-71 lineage—the random recombination framework put forth by McWilliam Leitch et al. or the adaptive mutation framework put forth by Tee et al. and Chen et al.—has powerful implications for vaccine development and control strategy. In the adaptive framework, EV-71 experiences antigenic drift similar to that observed of influenza and would require continuous antigen monitoring to keep vaccines up-to-date with pathogen evolution. In the recombination framework, seasonal immune escape is not guaranteed—but neither is accurate prediction of effective antivirals and therapeutics [23].

2. GLOBAL EPIDEMIOLOGICAL HISTORY

EV-71 was first isolated in California in 1974, from 20 patients who had manifested disease of the central nervous system (CNS), including meningitis, encephalitis, myocarditis and acute flaccid paralysis (AFP), between 1969 and 1974 [24]. BrCr, the prototype strain, was isolated from the stool samples of all 20 patients and from the brain of the only case fatality recorded in the outbreak, a five-year-old boy from Los Angeles County who died of encephalitis. Cross-neutralization and immunodiffusion tests demonstrated that BrCr was not related to any known enterovirus. Homologous neutralizing antibodies were also discovered in patients, indicating a causal relationship between the new enterovirus and the cases of severe CNS disease.

Figure 2 (from Bible et al. 2007) charts laboratory-confirmed epidemics of EV-71 from its identification in California in the 1970s through 2000. Following its debut in California, the virus appeared in an outbreak of aseptic meningitis in Melbourne, Australia in 1972. It was also implicated in an outbreak in New York State from 1972-77. Of the 28 New York patients, 19 presented with severe CNS disease.

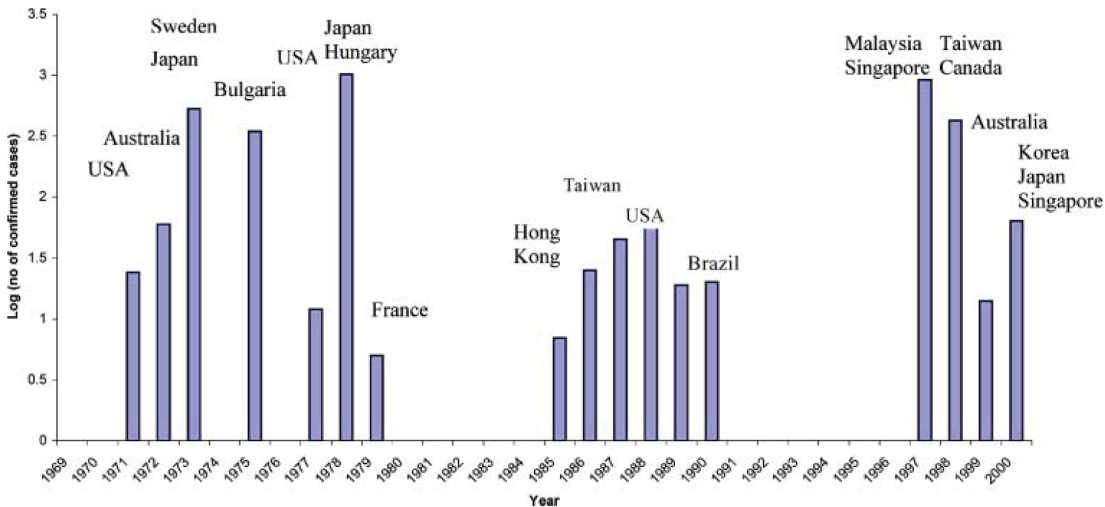


FIGURE 2: REPORTED EPIDEMICS OF EV-71 INFECTION, 1970-2000 (FROM BIBLE ET AL. 2007). Three separate waves of infection are identified, one in each decade. Only those epidemics with reported and laboratory-confirmed cases are shown.

High-fatality EV-71 epidemics were first reported in Bulgaria in 1975 and in Hungary in 1978, with 44 and 47 deaths respectively [25], [26], [27]. These two epidemics were noted for the overwhelmingly neurotropic disease presentation of their EV-71 strains. In the Bulgarian epidemic, 705 severe cases were recorded, of which 77.3% reported aseptic meningitis and 21.1% reported acute flaccid paralysis. The majority of those affected were under five years old. EV-71 was isolated from 25.3% of all clinically diagnosed cases and 100% of fatal cases. The Hungarian epidemic three years later saw 826 cases of aseptic meningitis and 724 cases of encephalitis. Of those, 17.6% of aseptic meningitis cases and 20.0% of encephalitis cases were caused by EV-71.

Interestingly, very few if any cases of HFMD or herpangina were reported in either the Bulgarian or Hungarian epidemics, despite their unusual size and severity. No cases of HFMD were reported in Bulgaria, while just four cases of HFMD associated with EV-71 infection were reported in Hungary.

2.1 EV-71 and HFMD

EV-71 was linked to HFMD for the first time in 1973, when outbreaks of HFMD in Japan and Sweden saw a small number of patients also present with severe CNS disease [9], [28]. Another HFMD outbreak with a small but significant number of cases presenting with neurologic sequelae occurred in Japan in 1978. Similar outbreaks continued into the 1980s, with outbreaks in Singapore and China in 1987 and in Melbourne, Australia in 1986 [29], [30], [7].

Large-scale epidemics of HFMD and severe CNS disease linked to EV-71 began occurring across the Asia-Pacific region in 1997, first in Sarawak, Malaysia in 1997 and then in Japan, peninsular Malaysia and Singapore in 1998 [2]. The Sarawak and peninsular Malaysian epidemics were the first to report a new severe CNS syndrome associated with EV-71 infection, a rapidly fatal pulmonary edema brought on by severe brain stem encephalitis [31]. The new CNS syndrome would also manifest in Taiwan.

2.2 The 1998 outbreak in Taiwan

When an outbreak of HFMD and severe CNS disease occurred in Taiwan in 1998, it was the largest EV-71 epidemic worldwide to date. Mild outbreaks had occurred in the small island country in 1980 and 1986, but the former had involved just 20 children in the northern capital city of Taipei and the latter had involved just four children in the southern city of Kaohsiung [4]. Globally, the previous largest EV-71 epidemic had been in Japan in 1978, when just over 30,000 cases were reported [32].

Sentinel physicians reported 129,106 total cases of HFMD and herpangina occurring in two waves (Fig. 3), the first spread over the entire island from March-July and the second confined mainly to the south from September-November [4]. Since the sentinel surveillance network involved just 9% of Taiwan's physicians, the unreported total incidence of HFMD/herpangina is estimated at roughly 1.5 million cases.

In a 2002 retrospective study of the 1998 outbreak, Chang et al. found that risk factors for infection in 1998 echoed the known fecal-oral route of enterovirus transmission and the virus's propensity for young schoolchildren. Individuals were at higher risk for infection if they had an older sibling or other family member with positive EV-71 serology before the epidemic, or if they were aged between 6 months and 3 years old [33]. Rural families were at higher risk, as they were posited to have more children in regular contact. Attending a kindergarten or other childcare center and drinking tap water was also found to increase risk.

EV-71 was isolated from two-thirds of all cases in the epidemic and, interestingly, from the vast majority of individuals presenting with severe CNS sequelae [33], [34]. Of the 405 severe neurologic cases, 78 were fatal. The majority of fatal cases experienced the rapidly fatal pulmonary edema syndrome that had been observed in Sarawak and peninsular Malaysia the year before.

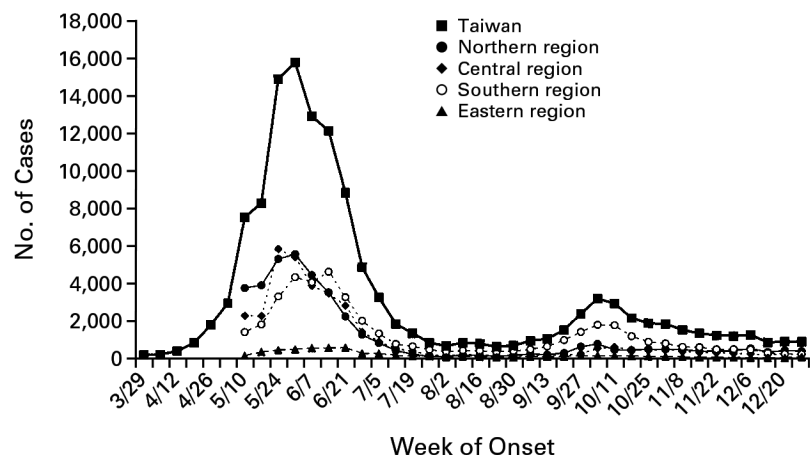


FIGURE 3: CASES OF HFMD/HERPANGINA REPORTED BY SENTINEL PHYSICIANS IN TAIWAN, MARCH-DECEMBER 1998 (FROM HO ET AL. 1999). Two epidemic waves are observed, the first from March-July and the second from September-November. The first is seen to have involved the entire island, while the second was concentrated notably in the south. Sentinel physicians comprise just 9% of the Taiwan's total physician population.

2.3 Recent activity

Following the 1998 Taiwan epidemic, EV-71 activity has continued in the Asia-Pacific region, with large outbreaks occurring in Perth, Western Australia, in 1999, in Singapore and southern peninsular Malaysia in 2000, and southeastern Australia in 2001 [2]. Outbreaks have also occurred in Japan, Vietnam and Cambodia. Each ensuing outbreak has seen a mix of dermatological and neurological symptoms.

In 2008, China saw its first large-scale epidemic of EV-71-associated HFMD. Over 10,000 cases were reported, along with 50 deaths among children [12]. Since then, the virus has continued to circulate and cause severe disease and death in the country, with 1705 total deaths reported from 2008-2011 [35].

3. QUESTIONS IN PATHOGENICITY

A key question in the study of EV-71 considers the range of disease caused by the virus. What causes one outbreak to manifest cases with primarily febrile, self-limiting dermatological symptoms, while another outbreak results in fatalities due to devastating neurologic illness?

No causal link between particular viral strains and particular symptoms has been identified. Ishimaru et al. found no antigenic differences between the prototypic BrCr strain, which caused strongly neurotropic symptoms in California in 1969, and the particular strains isolated from the 1973 and 1978 Japan epidemics, which mainly manifested dermatological syndromes [9]. Among the strains responsible for the epidemics in the Asia-Pacific region from 1997-2000, no clear “neurovirulent” strain has been identified, as at least three distinct genotypes were isolated from fatal cases in the 1997 Sarawak outbreak, the 1998 Taiwan outbreak, and similar outbreaks in peninsular Malaysia and Japan.

Working with the 1998 Taiwan epidemic, Yan et al. in 2001 presented three explanations for the differences in clinical presentations of infected patients: first, that two different EV-71 strains might be cocirculating; second, that minute changes in genetic determinants among the EV-71 strains might have caused different viral behaviors; or third, that coinfection with EV-71 and other pathogens like CA-16 might be manifesting severe disease [36].

4. COXSACKIEVIRUS-16

Genetically, EV-71 is most related to coxsackievirus-16, also a non-polio enterovirus in the *Picornaviridae* family [16]. The two enteroviruses are the primary causative agents of HFMD/herpangina. In many of the aforementioned outbreaks and epidemics involving both dermatological and neurological presentations, CA-16 has been implicated alongside EV-71.

It is important to note, however, that while HFMD and herpangina caused by CA-16 and EV-71 are clinically indistinguishable, only EV-71 has been clearly linked to severe CNS disease. Coxsackieviruses are known to primarily manifest mild dermatological symptoms like herpangina. In a 280-person study at a children's hospital in 2008, Chen et al. found that 18.6% of patients infected with EV-71 presented neurologic symptoms, while just 1.1% of those infected with CA-16 manifested CNS disease [37].

As to Yan et al.'s third explanation for differences in clinical case severity, co-infection with both EV-71 and CA-16 has not been studied in detail, but intriguingly, Chan and AbuBakar in 2004 found evidence of recombination between CA-16 and EV-71 strains in isolates from mild HFMD cases from the 1997 Malaysia outbreak [38]. Further study is necessary to investigate whether recombination between the two viruses results in a more or less virulent pathogen.

5. RESEARCH GOALS

It is clear from the background presented in this introduction that a great deal of work remains to be done to clarify the mechanisms behind the incidence of neurologic disease caused by EV-71. Ongoing research on the interaction of EV-71 and CA-16, the molecular epidemiology of the virus, risk factors for disease and the precise mechanisms of infection, pathogenesis and immune resistance will enable the development of better strategies for treatment and control.

Perhaps the most important of these ongoing advances is the effort to develop a vaccine. Inspired by the success vaccination has had in reducing the incidence of polio worldwide [39], this thesis seeks to characterize the true burden of EV-71 infection and to examine the effect vaccination could have using mathematical modeling. Previous HFMD modeling attempts have proposed continuous-time, deterministic compartment models [40]–[42]. Drawing on lessons from measles modeling, this thesis project seeks to instead utilize a discrete-time, stochastic model.

To that end, this thesis concerns itself with the incidence of EV-71 infection in Taiwan. As a nation with a readily available and well-attended surveillance system, Taiwan presents a potentially fruitful disease modeling opportunity. Since the devastating 1998 epidemic, cases of severe enterovirus infections have been reported in a publicly available database.

To delineate, the research goals are:

1. To analyze available data on the behavior of EV-71 in Taiwan;
2. To utilize a stochastic, discrete-time modeling approach to elucidate key epidemiological parameters from the data, including the unreported true burden of infection;
3. To use those parameters to model vaccination and estimate R_0 .

Methods

This section will be structured in two parts: first, a description of the dataset; second, details of the TSIR model. All analyses were conducted in R, using RStudio. Adobe Creative Suite was used to polish figures and Microsoft Excel was used for data cleaning.

1. DATA

The dataset captures confirmed cases of severe enterovirus infection in Taiwan from 1999-2013. After the 1998 epidemic, severe enterovirus infection became a class C notifiable disease in the national Notifiable Infectious Disease Surveillance System (NIDSS). Hospitals and physicians are required to report cases to the CDC within 24 hours of presentation [43]. Cases of severe infection are defined as a diagnosis of one or more of the following: a) myoclonic jerks, encephalitis, encephalomyelitis, acute flaccid paralysis, poliomyelitis-like paralysis, myocarditis, pericarditis, pulmonary edema or hemorrhage, or acute cardiopulmonary failure for patients of all ages, or b) thrombocytopenia, sepsis, hepatic failure or multi-organ failure for infants under 3 months of age. A panel of infectious disease specialists meets biweekly during the enterovirus peak season and monthly in the off-season to retrospectively discuss reported cases. Laboratory confirmation finalizes cases for inclusion in the dataset.

It is important to note that the dataset does not represent the total burden of infection. Only severe infections are reported to the NIDSS database. Data on the true incidence of enterovirus infection is difficult to collect since most infections manifest as self-limiting illnesses that do not require medical attention and consequently are not reported to health bureaus.

The raw data are available from the Taiwan CDC's NIDSS website.³ Cases are aggregated as counts of severe enterovirus infection, including disease caused by EV-71, CA-16 and other agents like echovirus. For mathematical ease, the data was adjusted such that all weeks with zero cases show one case. Demographic data published by the Taiwanese Ministry of Interior was used for additional analysis.⁴

2. MODELING

Epidemic models are used in the study of disease and control to forecast possibilities where practical or ethical constraints make experimentation impossible. As noted in Roberts & Heesterbeek 1993, models rely on oversimplification of actual disease conditions and behavior for mathematical ease and are thus not to be used as absolute quantitative predictors of disease behavior [44]. The process of fitting a real-world phenomenon to a model, however, often reveals underlying relationships between state variables or parameters that would otherwise be obscured.

The basic mathematical model of disease transmission is the Susceptible-Infectious-Recovered (SIR) compartment model. As outlined in Anderson & May 1992, the SIR model is a dynamic system that characterizes the flow of individuals between disease states according to a set of differential equations [44], [45]. A sample model schematic is depicted in Figure 4.

SIR models, which operate in continuous time, are typically applied deterministically, governed by parameters set at model initiation. The interplay between stochasticity and determinism represents a key debate in theoretical ecology, in particular the extent to which environmental or demographic stochasticity might shape ecological dynamics known to involve deterministic processes [46].

³ URL: <http://nidss.cdc.gov.tw/>

⁴ Demographic data can be found here:
<http://eng.stat.gov.tw/lp.asp?ctNode=2265&CtUnit=1072&BaseDSD=36>

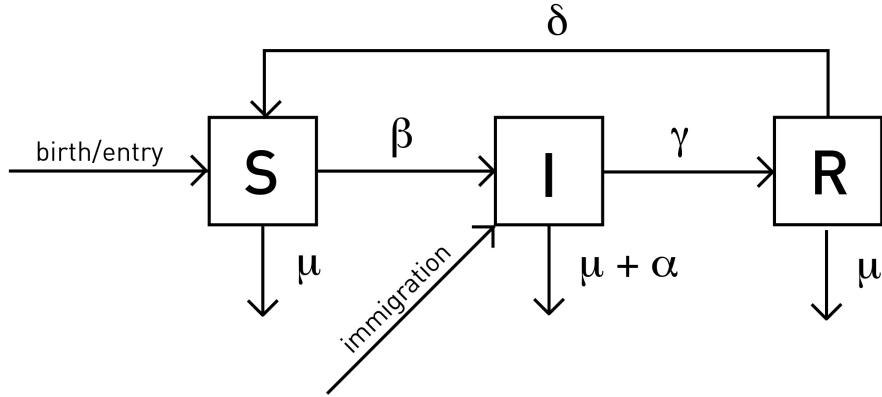


FIGURE 4: SAMPLE SIR MODEL SCHEMATIC (FROM TSENG 2013). Individuals flow between disease states S, denoting those susceptible to infection; I, denoting those infected and infectious; and R, denoting those who have recovered and are no longer infectious. Interactions between the compartments are governed by differential equations with parameters as shown.

2.1 The TSIR Model

The Time-series Susceptible-Infected-Recovered (TSIR) Model is a discrete-time, stochastic variant of the traditional continuous-time, deterministic SIR model. Developed by Finkenstadt & Grenfell in 2000, the model is intended for stochastic analysis of state variables reported in discretized units [47]. Bjørnstad et al. in 2002 performed a study of measles dynamics in the United Kingdom in which the TSIR formulation was used to capture stochastic dynamics of smaller population systems [48]. This project relied upon steps outlined in Bjørnstad's 2007 instructional text to inform attempts to parameterize and model enterovirus infection [49].

The TSIR model postulates that, given a discrete time step approximately equal to the generation time of the pathogen, it is possible to model the susceptible and infected classes in next-step units as such:

$$S_{t+1} = S_t + B_t - I_t \quad (1)$$

$$I_{t+1} = \beta S_t I_t^\alpha \quad (2)$$

Where S denotes numbers of susceptibles, I denotes numbers of infecteds and B denotes the number of births into the susceptible class. Parameter β denotes the transmission rate, and α denotes a “fudge exponent” used to smooth nonlinearities accumulated by discretizing an inherently continuous process and to capture heterogeneities in mixing during the contact process [47].

Λ_{t+1} denotes the expected value for next-step infecteds. The actual number of infecteds at next step, I_{t+1} , is assumed to follow a stochastic distribution around derived value Λ_{t+1} . For the purposes of this project, it was assumed that the actual number of next-step infecteds followed a negative binomial distribution as such:

$$I_{t+1} \sim NegBin(\Lambda, I_t) \quad (3)$$

With this doubly stochastic model for disease dynamics in hand, it becomes possible to use inference tools to derive necessary parameters from the dataset. Since the numbers represent only the most severe cases of infection, neither the value of S nor the value of I is known. The true susceptibles class might encompass the whole population, the child population or just a fraction without immunity. The true infecteds class might encompass all individuals with symptomatic or asymptomatic infection, or simply a subset of that class who experience symptoms somewhere between HFMD and severe CNS syndromes.

2.2 State variable reconstruction & parameter inference

In the presence of strong seasonal fluctuations in transmission rates and the absence of reliable records on true susceptible or infected populations, it becomes necessary to mathematically extrapolate from the dataset estimated figures for state variables to be used in parameter estimation. Such a process is termed “susceptible reconstruction.”

Let the true infecteds class I_t be given by:

$$I_t = \rho_t C_t \quad (4)$$

Where ρ represents the reporting rate and C represents reported cases. Where $\rho=1$, cases are fully reported; where $\rho > 1$, underreporting occurs.

Fluctuations in the susceptible class can be captured by the deviance of the true susceptibles course around a mean value. Given that $S_t = \bar{S} + D_t$, it follows that the deviance around the mean follows the same relationship as the total susceptible class. Thus (1) can be rewritten as:

$$D_t = B_t + D_{t-1} - \rho_t C_t \quad (5)$$

Or, when iterated:

$$D_t = \sum_{i=1}^t B_i + D_0 - \sum_{i=1}^t \rho_i C_i \quad (6)$$

Assuming a constant reporting rate, (6) can be written as the linear regression of cumulative reported cases against cumulative births.

$$\sum_{i=1}^t B_i = \rho \sum_{i=1}^t C_i + D_t - D_0 \quad (7)$$

Thus the slope of that regression follows as the reporting rate, and the residuals follow as the deviance of susceptibles around the mean. The derived reporting rate can be used to construct an accurate measure of next-step infecteds using (4).

The rest of the parameters can be elucidated again by means of linear regression. Recalling that $S_t = \bar{S} + D_t$, (2) can be rewritten as a regression of last-step infecteds against expected next-step infecteds:

$$\log(\Lambda_{t+1}) = \log(\beta_\mu) + \log(\bar{S} + D_t) + \alpha \log(I_t) \quad (8)$$

Transmission parameter β is here denoted as β_μ to recall its fluctuating nature. Minimizing the deviance of this regression derives the true mean number of susceptibles. With that value in hand, parameters β and α follow from a linear regression of $\log(A_{t+1})$ against $\log(I_t)$, with $\log(\bar{S} + D_t)$ as an offset.

2.3 Simulation

Once parameterized, the basic model outlined in (1), (2) and (3) can be used to simulate next-step susceptible and infected dynamics. The doubly stochastic nature of the model allows simulations to account for stochastic variability in predicted infecteds (3) and variable transmission rates (8).

Vaccination was introduced as a proportional variable, σ , added to the births term B in (1) to represent the proportional removal of a fraction of vaccinated individuals from entry into the next time-step's susceptibles class. Due to the discretized nature of the simulation, vaccination can be introduced at any step. Vaccination follows thus:

$$S_{t+1} = S_t + \sigma B_t - I_t \quad (9)$$

Of interest is the critical vaccination threshold, the proportion of population coverage after which herd immunity is achieved [50]. In a randomly mixed, homogeneous population, the critical vaccination threshold, p_c , can be used to estimate the basic reproduction number of the pathogen, R_0 , as follows [45], [51]:

$$p_c = 1 - \frac{1}{R_0} \quad (10)$$

This formulation assumes vaccination occurs at birth and is 100% protective. The basic reproduction number denotes the number of secondary infections produced by one primary infected individual entering a naïve population. Outbreaks are expected when $R_0 > 1$, and outbreak extinction is expected when $R_0 < 1$.

Results

This section will be structured in three parts: 1) a descriptive analysis of the dataset; 2) key parameters elucidated from the data; and 3) the results of a vaccination simulation.

1. DESCRIPTIVE ANALYSIS

Figure 5 depicts the time series of weekly severe case counts in the national population. In most peak years, epidemics occurred in multiple waves over the course of a 53-week year, capping weekly at 15-20 cases. Other years saw one spike in case incidence corresponding to just one wave of infection. Notably, the year 2008 saw cases peak just once: around weeks 24 and 25, which featured 38 and 39 cases, respectively.

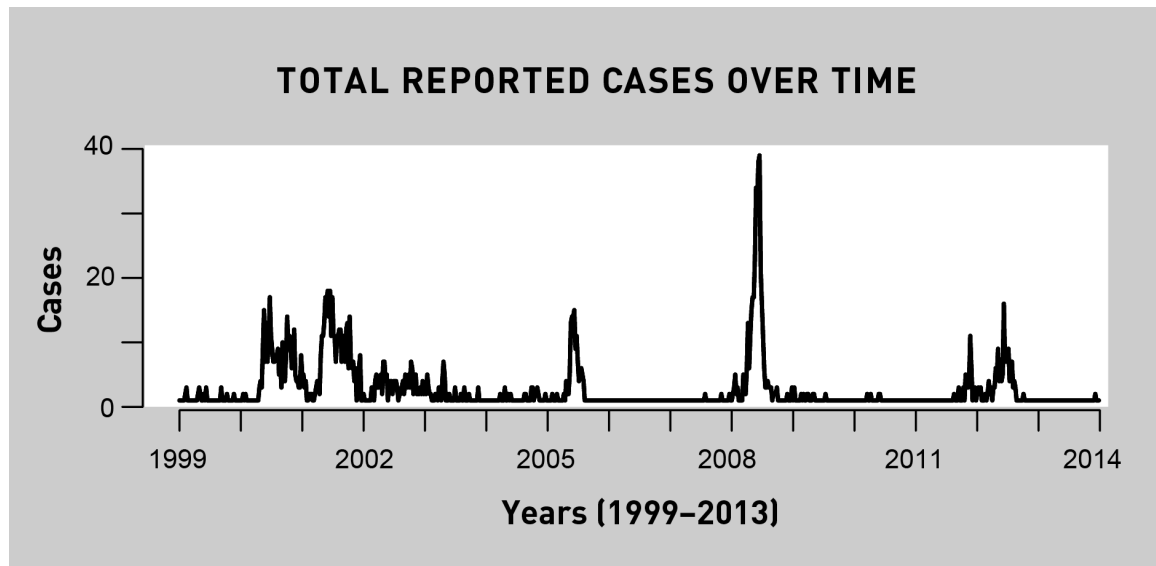


FIGURE 5: REPORTED WEEKLY INCIDENCE OF SEVERE ENTEROVIRUS INFECTION IN TAIWAN, 1999-2013. Epidemic or outbreak peaks are shown in 2000, 2001, 2005, 2008, 2011 and 2012. Data source: Case reports from the Taiwan Center for Disease Control's Notifiable Infectious Diseases Surveillance System (NIDSS).

1.1 Age distribution

Age distribution analysis of the reported cases shows that the vast majority of infections occurred in individuals below 2 years of age (Fig. 6). The age group from 0-2 years is shown to represent the highest proportion of total reported infections, with case reports slowing down through ages 2-4 and leveling off from ages 4+.

These results are consistent with the theory of enterovirus infection as primarily a childhood illness, transmitted via the fecal-oral route through schools and daycare centers [33]. Figure 7 shows that the age distribution remained apparently constant from year to year, with the age classes 1-2 years and 0-1 year consistently claiming the highest and second-highest numbers of cases, respectively.

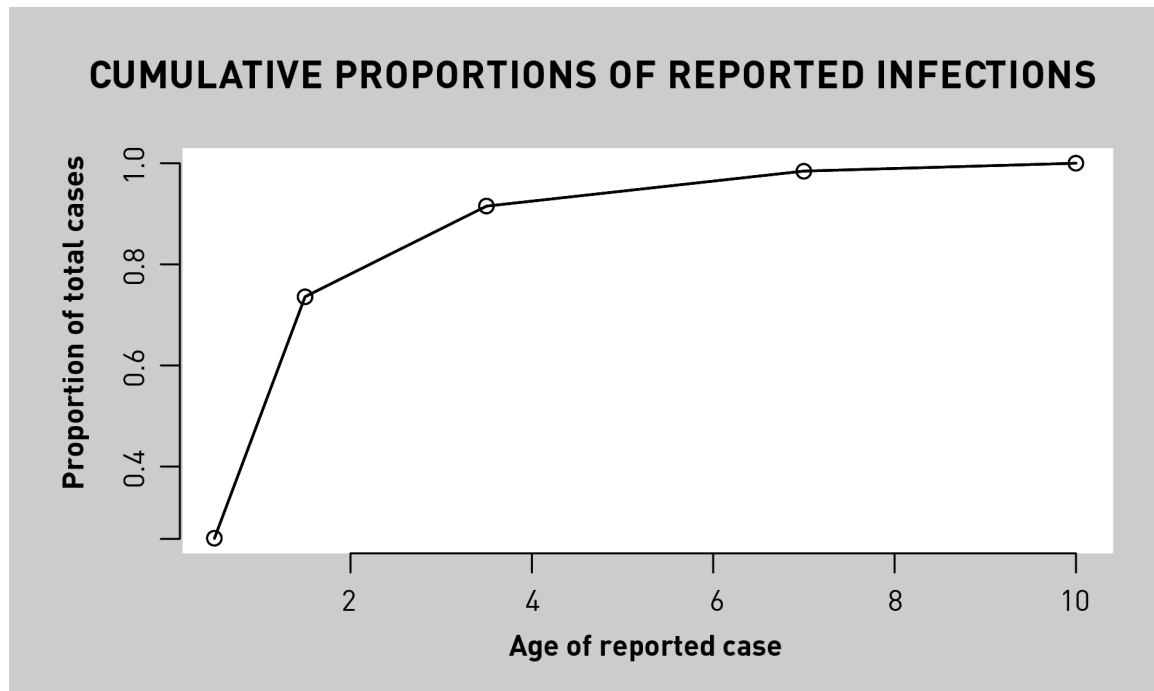


FIGURE 6: CUMULATIVE PROPORTIONS OF REPORTED INFECTION AT EACH AGE.

Infections are seen to accumulate most rapidly from ages 0-2.

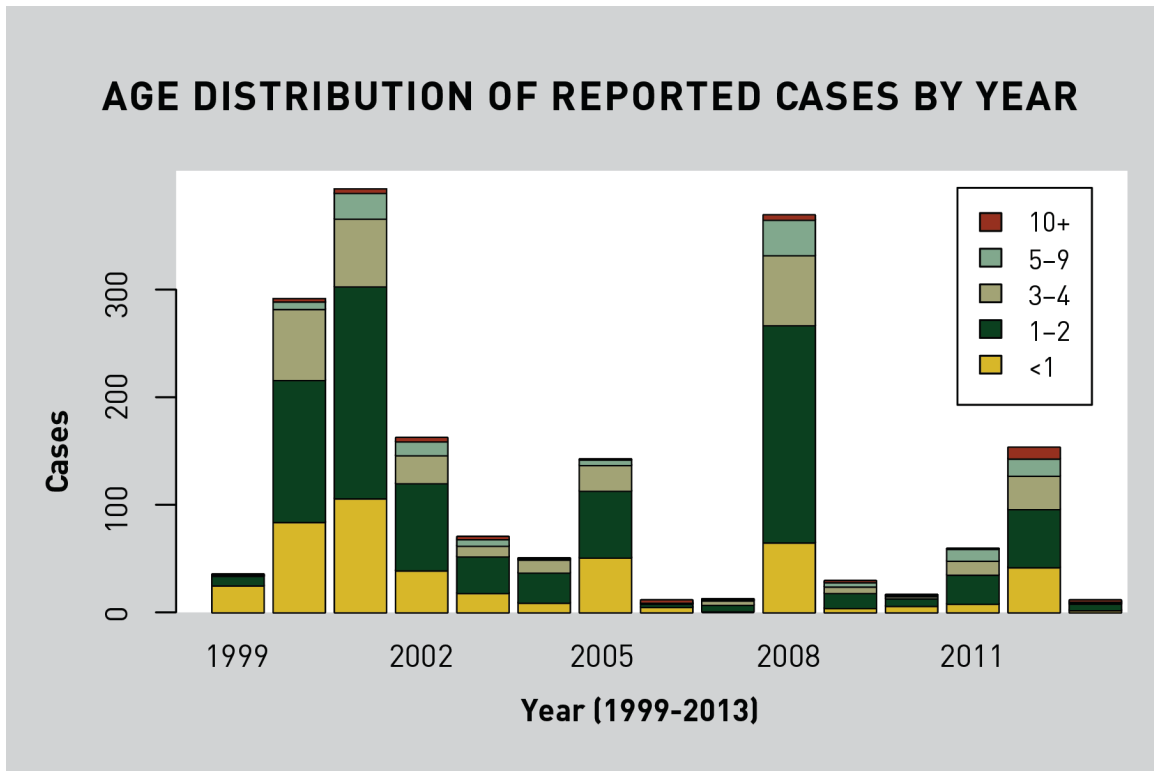


FIGURE 7: AGE DISTRIBUTION OF REPORTED CASES PER YEAR. The majority of reported infections are seen to occur in individuals under 2 years of age.

1.2 Seasonality

Seasonality in disease transmission is known to impact epidemic dynamics [52]. Models for measles, a similar childhood infection, have shown that seasonality in infection caused by school-term density forcing can play an important role in driving epidemic dynamics [48], [53]. In the case of measles, annual fluctuations in susceptible density brought on by the start and end of school have been implicated in creating environmental forcing that affects transmission rates. To investigate the role within-year fluctuations in susceptible density might have on overall epidemic dynamics, each of the 15 years in the dataset was plotted on a yearlong, 53-week axis (Fig. 8). Reported infections are seen to experience a trough in the first 10 weeks of the year and a peak around week 22, which roughly corresponds with the summer months.

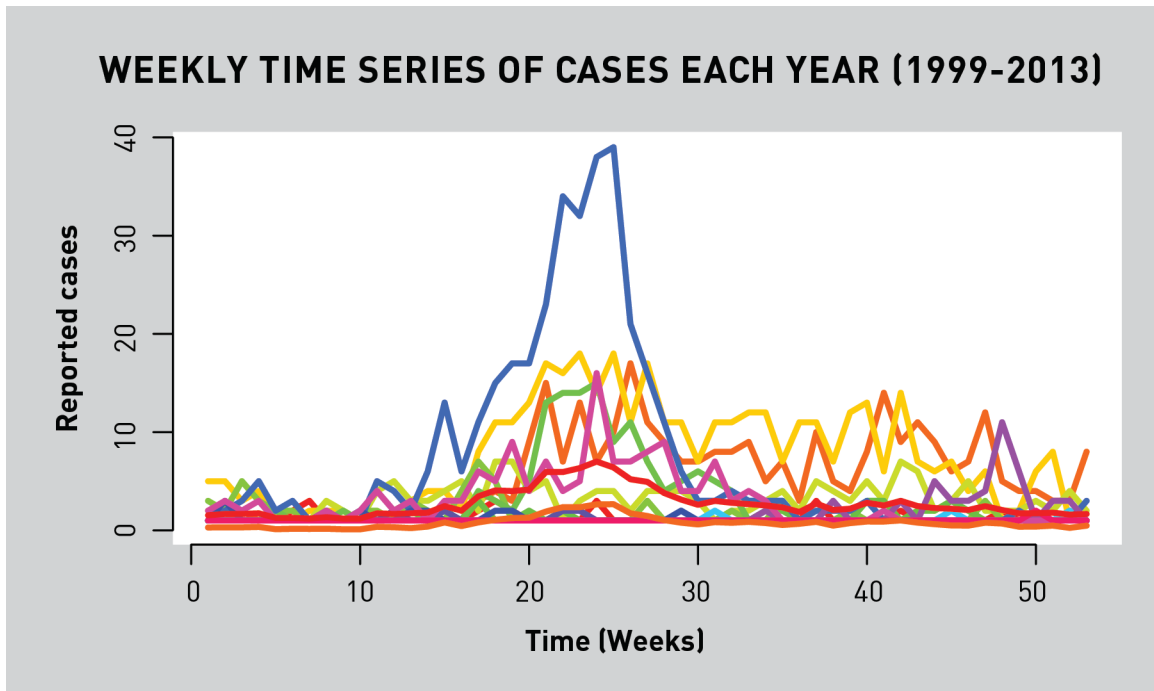


FIGURE 8: WEEKLY TIME SERIES OF CASES, BY YEAR. Each colored line represents the weekly course of infection for one of the fifteen years in the dataset. Reported infections are seen to experience a trough in the first 10 weeks of the year and a peak around week 22, which roughly corresponds with the summer months.

Unlike in the case of measles, the severe enterovirus infection data at hand does not display regular, periodically cyclic dynamics across the full time series. It is difficult to determine an interepidemic period from the fifteen years captured in the dataset.

To investigate the possibility of epidemic periodicity, the wavelet analysis developed by Grenfell et al. in 2001 [54] was applied (Fig. 9). The wavelet analysis uses autocorrelation functions to calculate serial correlations in a time series at different time lags and periodogram spectral analysis to examine the time series in terms of waves of different frequencies, with the importance of each frequency measured by spectral amplitude. The wavelet analysis was unable to locate sustained epidemic periodicity across the time series, suggesting that there is none. This may be due to the relatively short time over which data has been collected, or to the fact that the data represents a very small subset of total epidemic activity.

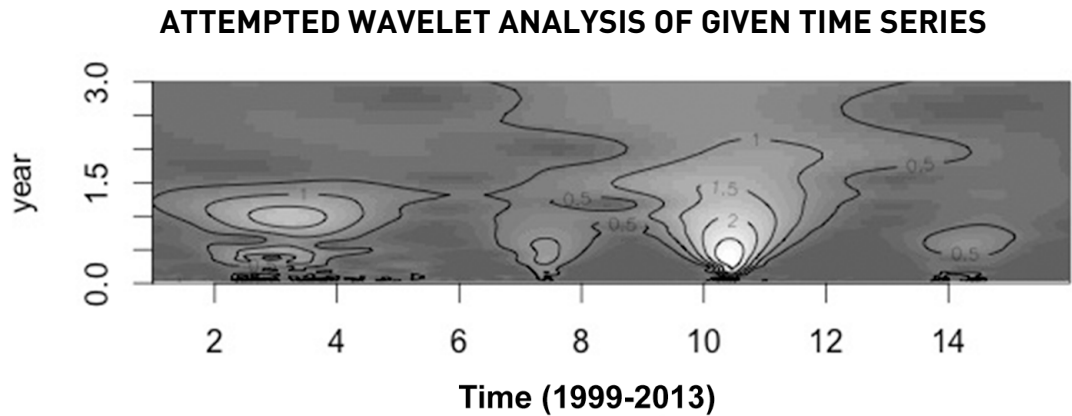


FIGURE 9: WAVELET ANALYSIS OF EPIDEMIC PERIODICITY. The lack of clear periodicity in the time series is shown.

2. PARAMETER DERIVATION

The key results of the model fitting performed in this section are reported in Table 1. A number of assumptions were utilized in the modeling process to optimize the real-world data for mathematical application. This section will discuss in depth the modeling processes of each parameter derivation.

TABLE 1: KEY DERIVED PARAMETERS

Parameter	Result	
	Value	Related figure
Transmission parameter (β)	See Table 2 (Appendix)	
Contact parameter (α)	0.8316127	Fig. 14
Mean number of susceptibles (\bar{S})	4383.252*	Fig. A3
Mean reporting coefficient (ρ)	1492	Fig. A2
Model fit	$m = 1.000025$	Fig. 12

* For inference purposes, the susceptibles class was narrowed, first to 15.65% of the total national population of 23.34 million, corresponding to the national under-15 population, and then 0.01-1% of that population, corresponding to a very small minority of individuals likely to develop life-threatening neurological illness.

Transmission parameters β were found to fluctuate seasonally as expected. While the magnitude of seasonality evidenced in the derived parameters was overall not very significant, due perhaps to the sparseness of the dataset, the derived parameters do appear to map onto the reported infecteds course. Figure 10 depicts the weekly course of transmission parameters and the weekly course of infection for one year, averaged between all 15 years. Transmission is seen to peak just before week 20, corresponding with the months of March and April, and again at around week 35, corresponding with the month of September. The first of these peaks falls in line with the start of the humid season in Taiwan, and the second falls in line with the start of school.⁵

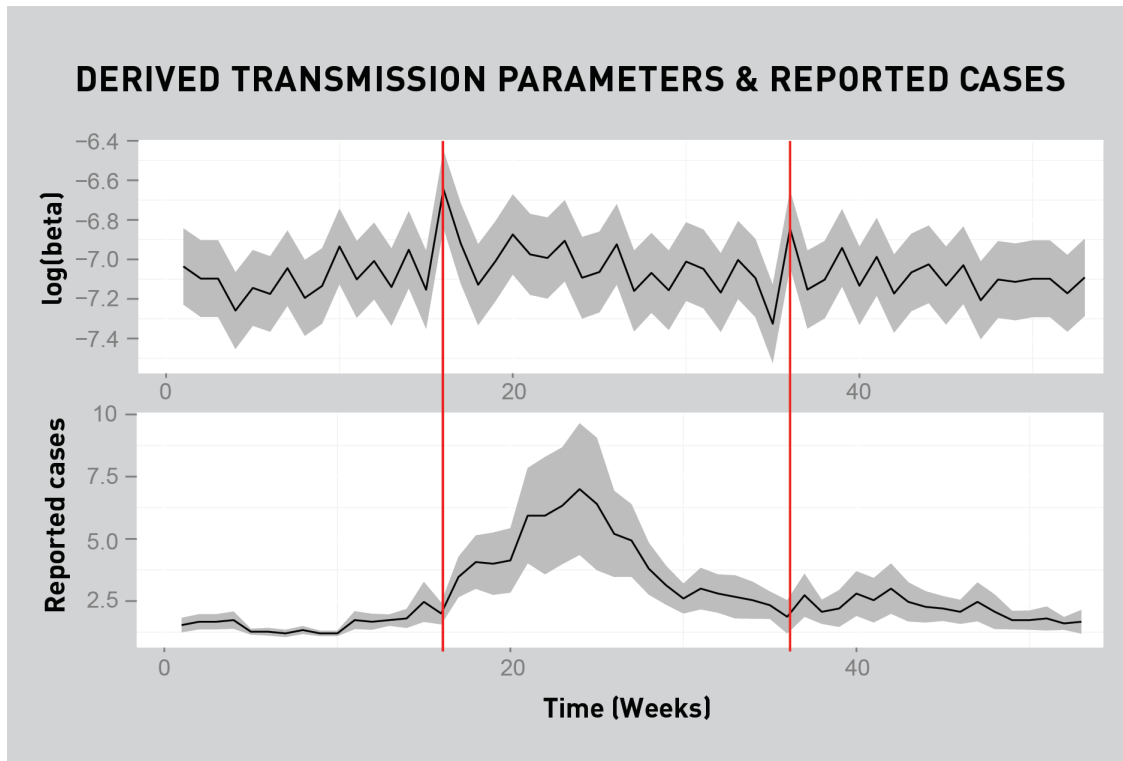


FIGURE 10: AVERAGE WEEKLY COURSE OF TRANSMISSION AND INFECTION. Top: Derived weekly course of transmission. Bottom: Average weekly course of reported cases. Gray areas represent error bars \pm one standard deviation. Red lines indicate peaks of the derived transmission course.

⁵ Source: Personal correspondence with relatives in Taiwan.

2.1 Underreporting

Figure A1 (Appendix) depicts the regression of cumulative cases against cumulative births. A massive tendency towards underreporting is demonstrated, with a mean p-value of 1492. This massive underreporting tendency fits within the bounds of the data: as stated previously, the dataset captures only the most severe cases of infection, the ones causing neurologic symptoms that warrant hospital or physician visits. Figure 11 (Appendix) depicts the time series of reporting rates derived at each timestep. While reporting rates were assumed to hold constant for the purposes of mathematical inference, it appears some fluctuation does exist.

2.2 Susceptible reconstruction

In proposing candidate mean susceptible values as part of susceptible reconstruction, a number of adaptations to the TSIR model were made in order to accommodate biological features of HFMD and systemic features of the dataset. Since severe enterovirus infection commonly manifests in children under the age of 15, a demographic that comprises 15.65 percent of the Taiwanese population, a scaling factor p was set at .1565 and applied to the total population size to produce a population pool consisting only of children under 15.

From this population pool, serology studies in the literature are typically used to narrow down a proportion of the total population that can be considered candidate susceptibles. But in the case of this project, literature estimates of percent seropositivity could not be used to derive a candidate susceptible population proportion, since most infections result in mild disease not captured in the dataset and since it is unclear why certain individuals progress to severe disease. For the purposes of mathematical inference in this study, it was assumed that between 0.01-1% of the population pool of

under-15s could be construed susceptible to developing the severe neurologic symptoms represented in the data.

The final adjusted mean susceptible value, 4383.252, was identified as the candidate value with the minimal deviance (Fig. A3). From this value and the derived deviance course over the 795 time-steps in the dataset, a susceptibles course was reconstructed. The relative dimensions of the reconstructed susceptibles course appear promising: as seen in Figure 11, the reconstructed time series of susceptibles appears to map onto the time series of reported cases.

For all epidemic or outbreak years, susceptibles are seen to build up in the interepidemic interval before crashing at epidemic onset. Epidemic years in which cases were spread out in waves show slower gradations of susceptible crashing, while epidemic years like 2008 in which all activity occurred in one peak depict one rapid crash.

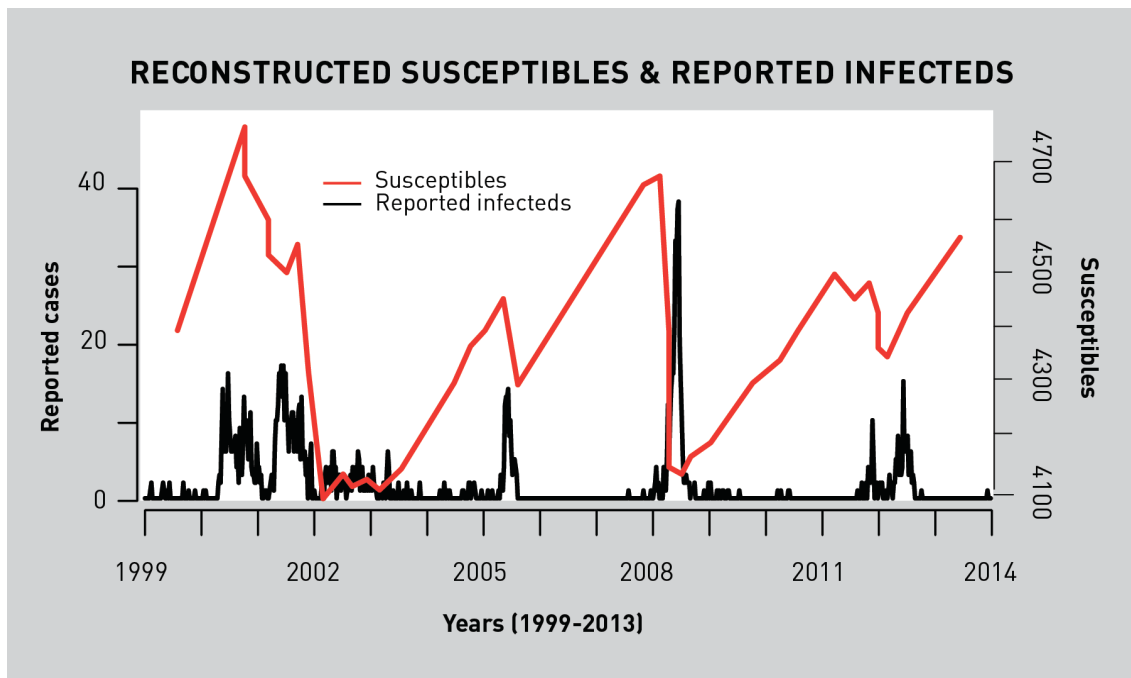
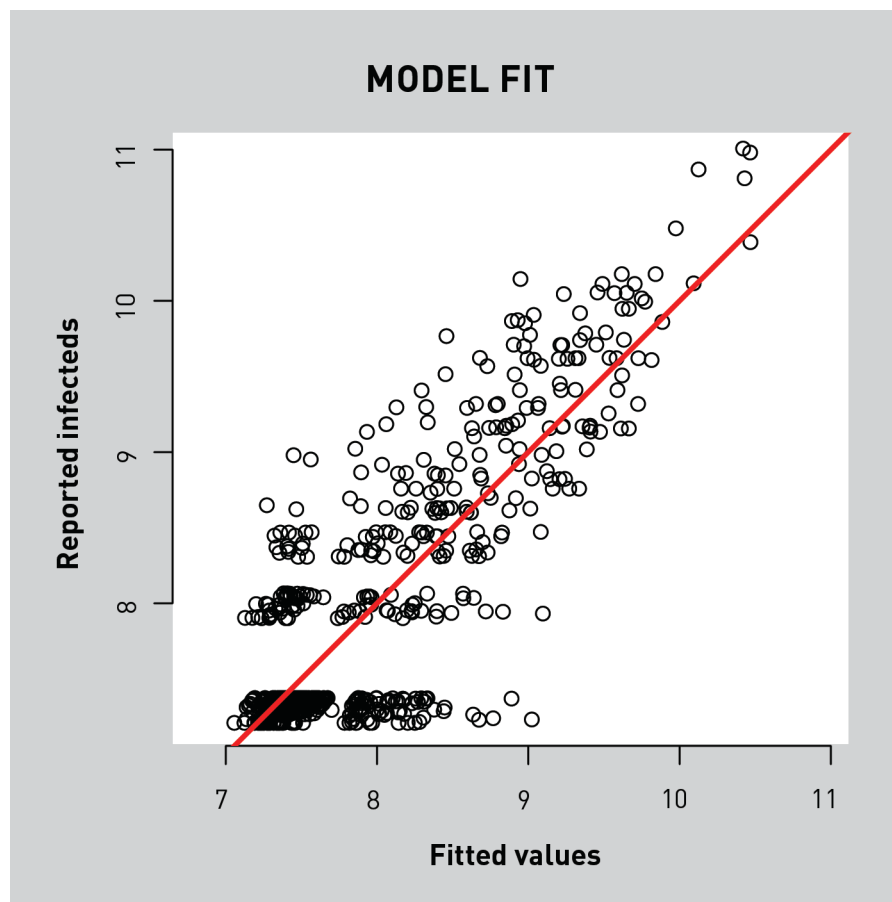


FIGURE 11: RECONSTRUCTED SUSCEPTIBLES (IN RED) AND REPORTED INFECTEDS (IN BLACK). Susceptibles are seen to build up before crashing at epidemic onset.

Interestingly, at the 2005 epidemics, susceptibles did not crash fully down but instead dipped before climbing back up, only to crash fully in 2008. The data is not robust enough to predict cyclic dynamics, but preliminary observation indicates a similar dip-down may have occurred in 2012, perhaps forecasting a full crash in 2015.

2.3 Model fit

In order to examine model fit, the predicted values for $\log(I_{t+1})$ produced by the regression function were themselves regressed against the log-values of actual next-step infecteds reported in the dataset. The resulting correlation indicates the extent to which the model accurately captured the dynamics of the reported time series. With a slope of 1.000025, the correlation indicates the model fit successfully.



**FIGURE 12:
MODEL FIT.**
Fitted values for infecteds predicted by the model plotted against actual values for infecteds observed in the dataset. The slope of the regression line was 1.000025, indicating a near-perfect correlation.
 $R^2 = 0.7215$

3. SIMULATION

Once parameterized, the model could be used to forecast a time series of infecteds based on next-step predictions. When simulations were run using the derived β and α parameters, and with births set as a vector of actual demographic data, the simulated infecteds course blew up to epidemic proportions before crashing back to low endemic-like levels just after 250 time-steps (Fig. 13).

Figure 14 shows the effect of varying contact parameters (α) on the course of simulated infecteds, with transmission parameters set as the derived course and births set as the true data. Extreme crashes are seen in the simulations at $\alpha=0.8321$ (the derived value) and $\alpha=0.85$, as well as near the end of the course at $\alpha=0.90$, while the simulation at $\alpha=0.80$ shows regular oscillations rising and falling with the births input.

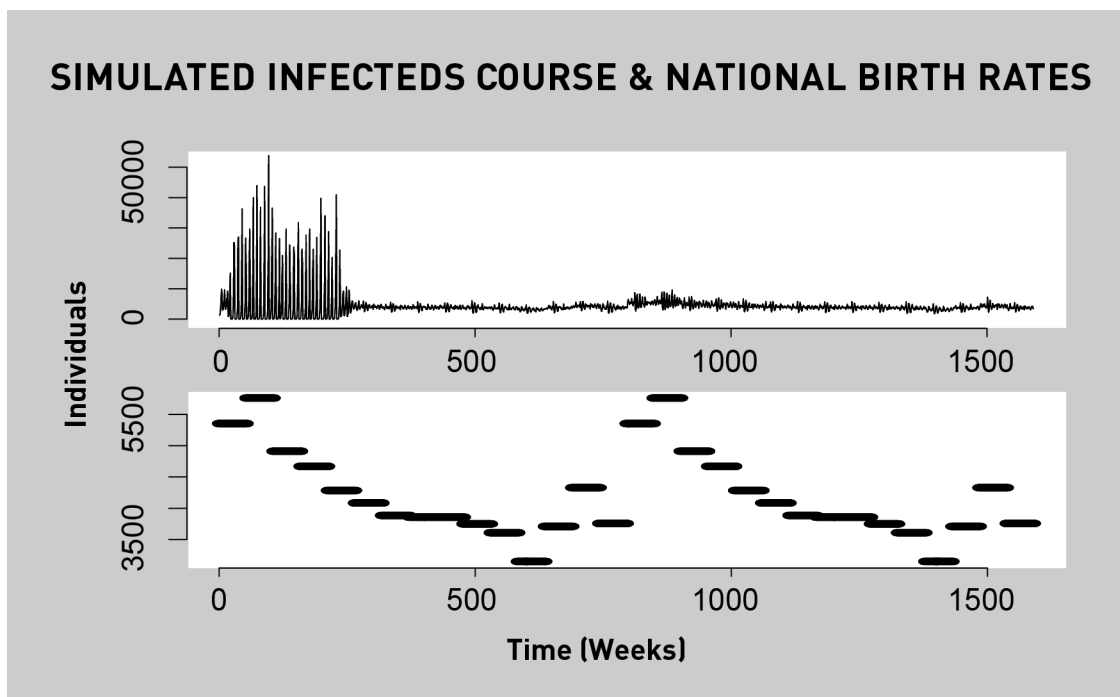


FIGURE 13: SIMULATED TIME SERIES OF INFECTEDS USING NATIONAL BIRTH RATES FROM 1999-2013. Top: Simulated infecteds course. Bottom: Corresponding birth rate inputs drawn from demographic data from 1999-2013 and repeated to generate a 30-year (1590-week) simulation.

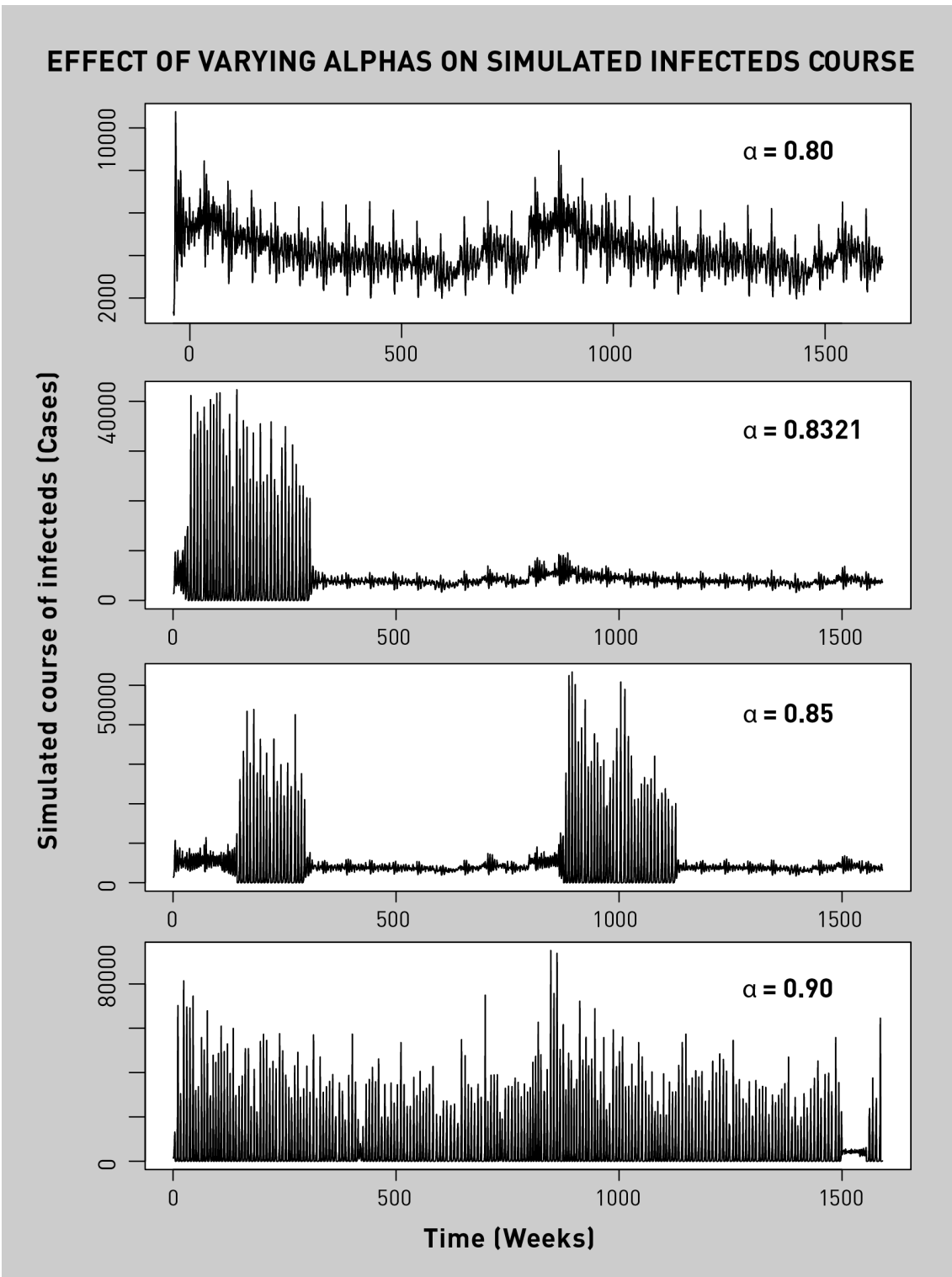


FIGURE 14: SIMULATED TIME SERIES OF INFECTEDS AT VARYING CONTACT PARAMETERS. Each simulation was run according to the alpha indicated, with transmission parameters and births set at the derived values and the values gleaned from demographic data, respectively.

4. VACCINATION

In the interest of generating a course of regular, periodic dynamics for vaccination simulation, births were set at a constant baseline rate (4197.765 births/week) representing the mean birth rate from 1999-2013. As seen in Figure 15, simulated disease activity both pre- and post-vaccination is characterized by periodic fluctuations that remain relatively constant through the time series after an initial boom. Vaccination is shown to result in a prompt, rapid decrease in the infecteds course down to a stable level of infection that persists at regular, constant fluctuations until endpoint. This pattern did not change when different vaccination times were introduced.

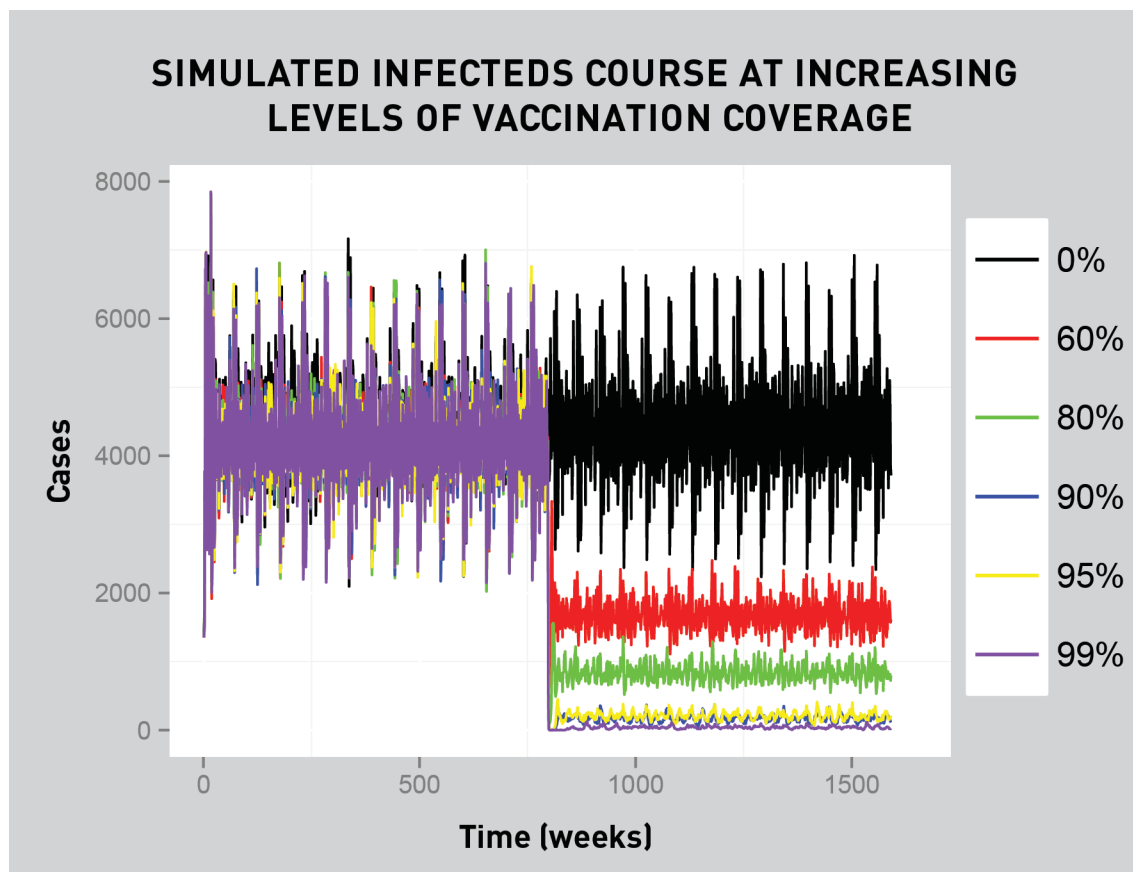
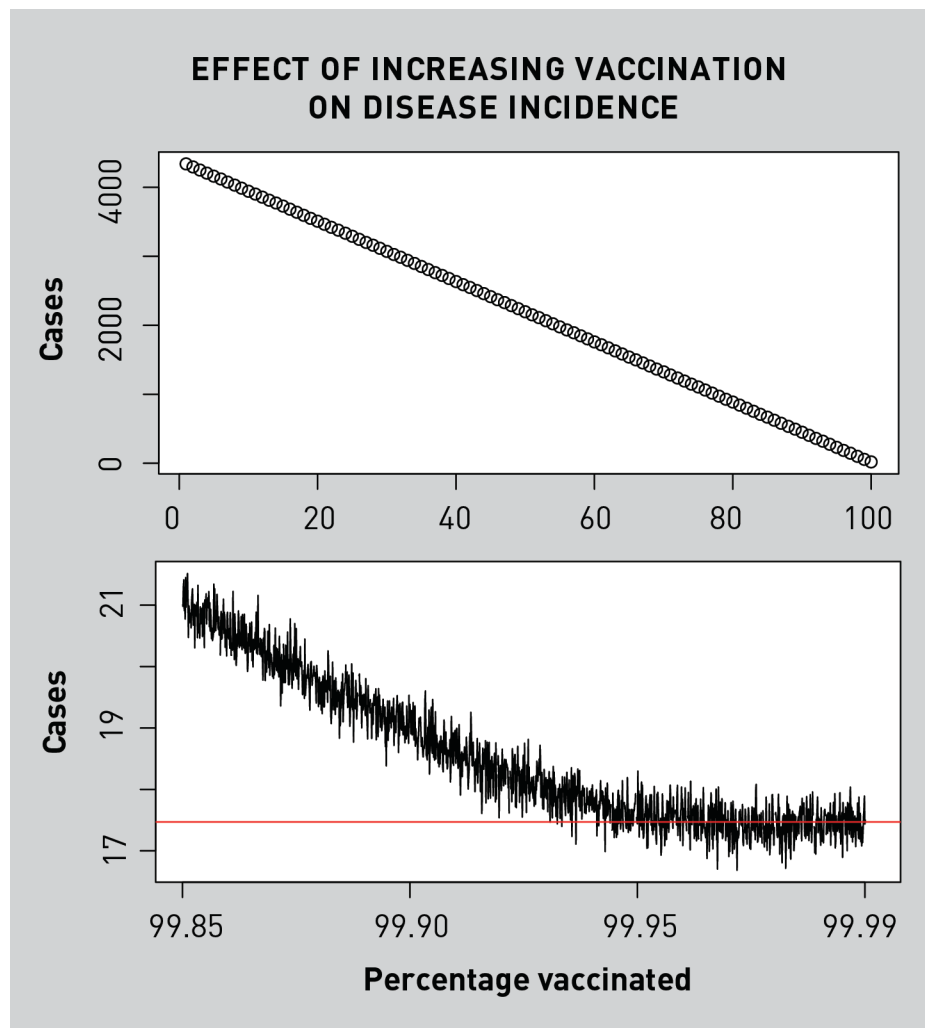


FIGURE 15: TIME SERIES OF SIMULATED INFECTEDS AT INCREASING LEVELS OF VACCINATION COVERAGE. Each color represents a different level of vaccine coverage. For each simulation, vaccination was introduced at the midpoint of the time series. Transmission and contact parameters were set at derived values.

Since vaccination appeared to promptly produce a dramatic reduction in the total population burden of disease, the effect of increasing vaccine coverage could be measured as the mean of the cases from vaccination to endpoint. The resulting plot shows a negative linear relationship between the percentage of the population vaccinated and the mean number of cases post-vaccination.

Interestingly, the downward trend levels off into a horizontal asymptote (cases=approx. 17.5) when vaccine coverage hits 99.95% of the population. This is tentatively interpreted as a critical threshold for vaccination, p_c , and a tentative R_0 of 2000 is elucidated from the simulated data.



**FIGURE 16:
EFFECT OF
INCREASING
VACCINATION
COVERAGE ON
DISEASE
INCIDENCE.**
A strong negative linear relationship is observed between high percentages of the population vaccinated and reduced numbers of infected cases. The relationship levels off at 99.95% coverage.

Discussion

This section will discuss in three parts: 1) key results, 2) challenges faced in the course of modeling, and 3) recommendations and future directions for research.

1. KEY RESULTS

1.1 Transmission parameters (β) successfully derived

This project has evidenced the usefulness of the TSIR approach in extrapolating parameters to characterize a time series of reported infection. In particular, TSIR is shown to be effective on datasets with very small case counts. The model fit shown in Figure 12 and the fit of reconstructed susceptibles on reported infecteds shown in Figure 11 demonstrate that the approach was able to characterize the reported infecteds course. Further bolstering this result, Figure 10 shows that transmission peaks correspond with peaks in reported infecteds. The peak in late March/early April corresponds with the start of the humid season, and the peak in September corresponds with the beginning of the school term. Wang & Sung in 2005 found no significant correlation between weather patterns and case reports of severe infection, but the transmission parameters elucidated in this study provide a novel result for analysis [42].

The success of the derived parameters is dampened, however, by the observation that they do not exhibit substantial seasonality. This can be attributed to the irregularity of the dataset. Finally, Figure 9 shows a delay between transmission peaks and case report peaks, suggesting a latent period between infection and reporting of serious disease. This delay cannot be construed as a latent period, however, as delays in reporting and in the manifestation of severe symptoms may be responsible for the lag.

1.2 Contact parameter (α) successfully derived

As seen in equation (2), the parameter α is a “fudge factor” used to smooth the discretization of an inherently continuous process. It also captures heterogeneities in the contact process. As α approaches 1, mixing approaches homogeneity [47].

In this project, α for the dataset was calculated to be 0.8316127, with a standard error of 0.02047 and a t-value of 40.63. The result may indicate the presence of a degree of heterogeneity in the contact process of transmission, but due to the comparatively low t-value associated and the behavior of the simulation at the derived contact parameter (Fig. 14), it is to be considered a rough approximation. It seems likely, though, for a virus transmitted via the fecal-oral route that some susceptibles would be more likely to contract disease than others.

1.3 Simulations produced

The infecteds course simulated by the model does not map onto the data from which its parameters were extrapolated. This is not surprising, since the dataset used in this project is known to constitute a small proportion of the true burden of enterovirus infection. One of the critical assumptions of the model was that transmission parameters might be elucidated from available case counts that could forecast cases not captured in existing data. One can imagine a proverbial iceberg’s worth of self-limiting, mostly febrile infections, mild HFMD/herpangina infections and even unreported severe infections that are not recruited into the dataset.⁶ The vaccination simulation that follows from baseline forecasting must be taken with the caveat that it is not possible to determine whether the simulated course represents the true burden of infection, since current surveillance systems do not capture those figures.

⁶ In the 1998 epidemic, as stated previously, the unreported total number of HFMD/herpangina cases is estimated at 1.5 million. The number of severe infections reported to hospitals was 405.

The simulation shown in Figure 13, however, is surprising. The dramatic decrease in simulated infections at a seemingly arbitrary point in the time series has no readily apparent biological explanation. The analysis shown in Figure 14 demonstrates that the epidemic crashing may be due to the effect of the contact parameter: between 0.80 and 0.85, the range in which the derived parameter falls, epidemic crashing is observed. As the value of the contact parameter approaches 1, infecteds dynamics smooth out to more regular, periodic cycles, but crashing still occurs. A more robust dataset might provide a more accurate approximation of the contact parameter, which might produce better simulations.

1.4 Vaccination modeled

The negative linear relationship found between increasing vaccination coverage and mean number of cases at endpoint fits within the framework put forth by the model [45]. The simulation has treated the entire national population as one randomly mixed patch and assumed population-wide, untargeted control, eliminating individual dimensions of heterogeneity in its assumptions of transmission potential.⁷ Increasing vaccination coverage is assumed to levy control equally across each individual in the population patch, and thus the linear relationship elucidated fits.

The asymptotic behavior of the relationship beginning at 99.95% vaccination coverage, however, is of note. Given constant births and the introduction of vaccination in the middle of an established, periodic epidemic course, it appears impossible to eliminate infection in the population. The asymptote can be also construed as a critical vaccination threshold, p_c .

⁷ Lloyd-Smith et al. in 2005 showed an important role for individual heterogeneity in transmission and contact rates in determining the course of a population-level epidemic, in particular the role of superspreaders [58]. The data available in this study did not afford the possibility of individual-level analysis.

From equation (10) and a p_c value of .9995 derived from the simulation, R_0 for the disease is estimated at 2000. This should not be construed as a realistic estimation of the basic reproduction number of enterovirus-71, given that the model fit here is a rough approximation based on a dataset of severe infections known to contain cases caused by more than one virus, and given that this interpretation would mean one enterovirus-infected child is able to infect 2,000 close contacts. It can be taken as an indication, however, that the reproduction number of the virus is likely high.

2. CHALLENGES

The limitations of available data presented a critical challenge to this project. As stated previously, the dataset at hand captured a very small proportion of total infection. Additional case counts of mild EV infection from sentinel and laboratory surveillance systems, such as those used in Chan et al. 2014 [55], might have provided a more robust dataset and a more realistic analysis. At the very least, a more robust dataset might have provided a window into whether enterovirus infections follow the periodic, cyclic dynamics observed in measles.

To further complicate this analysis, the dataset is known to aggregate all cases of severe enteroviral infection in Taiwan, not just those caused by EV-71. While the interaction between EV-71, CA-16 and other known etiologic agents of severe CNS disease like echoviruses has not been fully teased out, it is known that EV-71 is the primary agent behind severe disease. It can be construed that the elucidated parameters represent the behavior of EV-71, and that the simulated case counts represent unreported EV-71 infections; however, vaccination and control conclusions drawn from this study must take into account the reality of interaction between distinct viruses, among other assumptions of the model.

2.1 Modeling assumptions

An ever-present challenge of all theoretical disease modeling is the threat that the assumptions made for the purposes of mathematical inference make it difficult to map results onto observed conditions. Every effort is usually made to create model conditions that closely mimic observed conditions, but this project faced several unusual challenges attributable to the newness of the virus and a relative lack of research into its epidemiology and biology.

Critically, this project suffered from a lack of clear consensus in the literature as to serological estimates of EV-71 susceptibility. While serological estimates alone would not have clarified susceptible reconstruction owing to the fact that it is not known which individuals to include or exclude from the possibility of severe enterovirus infection, susceptibility estimates would have benefited from clearer consensus.

Huang et al. in 2012 found that in 2006, 20% of children in a public kindergarten in Taipei were seropositive for EV-71 exposure. That number decreased to 6% in 2007 [56]. Chang et al. in 2002 found a wide range of seropositivity among age ranges. Their results also suggest that an individual's likelihood of inclusion in the susceptible class also depends strongly on whether he or she has an older sibling with a history of illness [33]. Seropositivity and, therefore, immunity to infection also appears to vary according to time from the last epidemic.

The highly variable nature of seropositivity made it difficult to propose candidate mean susceptible values in the modeling process. The mathematically convenient assumption was to narrow the total island population to the proportion of individuals under 15, and then to 0.01-1% of that figure. These assumptions are neither supported nor refuted by existing knowledge.

The vaccination analysis conducted in this project also utilized a number of assumptions for mathematical convenience. Vaccination was assumed to deliver 100%

immunity, eliminating the need for a parameter governing vaccine efficacy. Loss of immunity was not factored into the vaccination simulation because it was assumed to be biologically irrelevant: EV-71 primarily affects children, suggesting that by adulthood, natural immunity has built up such that loss of vaccination immunity would not result in a return to the susceptibles class. As stated previously, the model also assumed vaccination would occur en masse to a homogeneous population of randomly mixing persons, sidestepping the issue of individual-level heterogeneities in transmission.

As stated previously, it was assumed that the dataset captured just EV-71 infections. Co-infection or cross-immunity due to the interaction of multiple viral strains or species would complicate a simulation and, more critically, a vaccination effort targeted at a single serotype. The vaccination simulation also did not take into account the fact that individuals might develop symptoms from the vaccine. As seen in the case of the oral poliovirus vaccine, vaccine-associated paralytic symptoms and the circulation of vaccine-derived poliovirus can result from the dissemination of a live, attenuated enteroviral vaccine [57].

3. FUTURE DIRECTIONS

This study utilized an underreported dataset of case counts to extrapolate parameters then used to theoretically simulate what might be the true, underreported burden of infection. Through the course of working with this dataset, a number of prospective directions for more accurate, full-throated research emerged.

First and foremost, existing datasets must be improved if modeling efforts are to continue. More stringent surveillance programs and more publicly available data might provide the materials necessary to gauge the accuracy of existing modeling attempts and to use more sophisticated modeling approaches to forecast control. A modeling effort on

a dataset that included all EV-71 infections, not just those manifesting severe symptoms, might yield more realistic results.

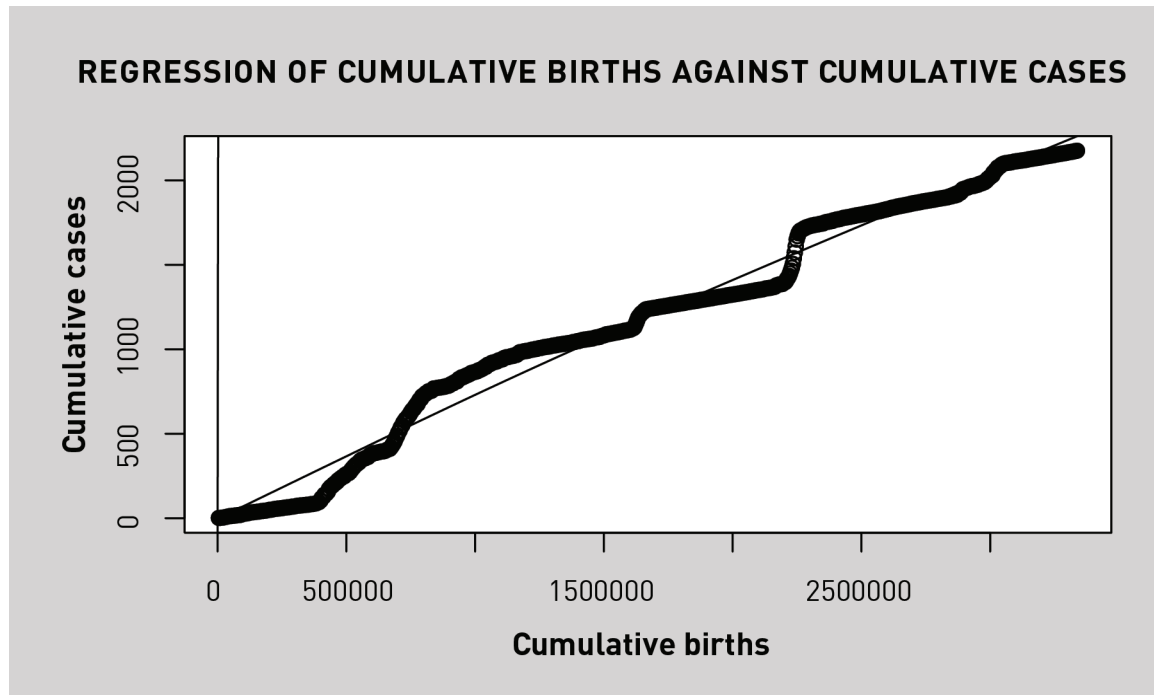
While the stochastic, discrete-time model utilized in this project was able to characterize the existing data to a degree of success, the limitations of the model were such that vaccination was modeled with a grossly oversimplified scheme. Deterministic, continuous-time compartment models governed by differential equations provide a malleable framework for more complex control strategies than the percentage-based vaccination coverage analysis carried out here. A tantalizing area of future study would be to fit a governing equation to the transmission parameter course elucidated in this study, which could then be used to parameterize a deterministic, continuous-time model.

Finally, research on the epidemiological behavior of EV-71 in Taiwan would benefit from a clarification of the spatial dynamics of contact and transmission on the island. Such research could characterize heterogeneities in transmission that would be vital to effective control measures. Work has been done examining spatio-temporal clusters of infection based on geographic data aggregated by existing surveillance [55], but network-based models identifying target populations might prove more useful for a childhood illness known to spread most effectively through schools.

The findings of this project provide at the very least an interesting application of the TSIR model to an emerging childhood infection less well studied than measles or polio. As EV-71 continues to cause epidemics of disease with wide-ranging, seemingly random severity all over the Asia-Pacific region, researchers daily draw closer to the prospect of a successful vaccine. Epidemiological models like this that are able to capture disease incidence and forecast the prospective effect vaccination could have on population dynamics will be necessary for the safe implementation of proper control strategies.

Appendix

FIGURE A1: REGRESSION OF CUMULATIVE BIRTHS AND CUMULATIVE CASES



The vertical line represents a $y=x$ line, showing the very small slope of the regression line. The slope of that line is an indication of the reporting parameter.

FIGURE A2: DERIVED REPORTING RATES OVER TIME

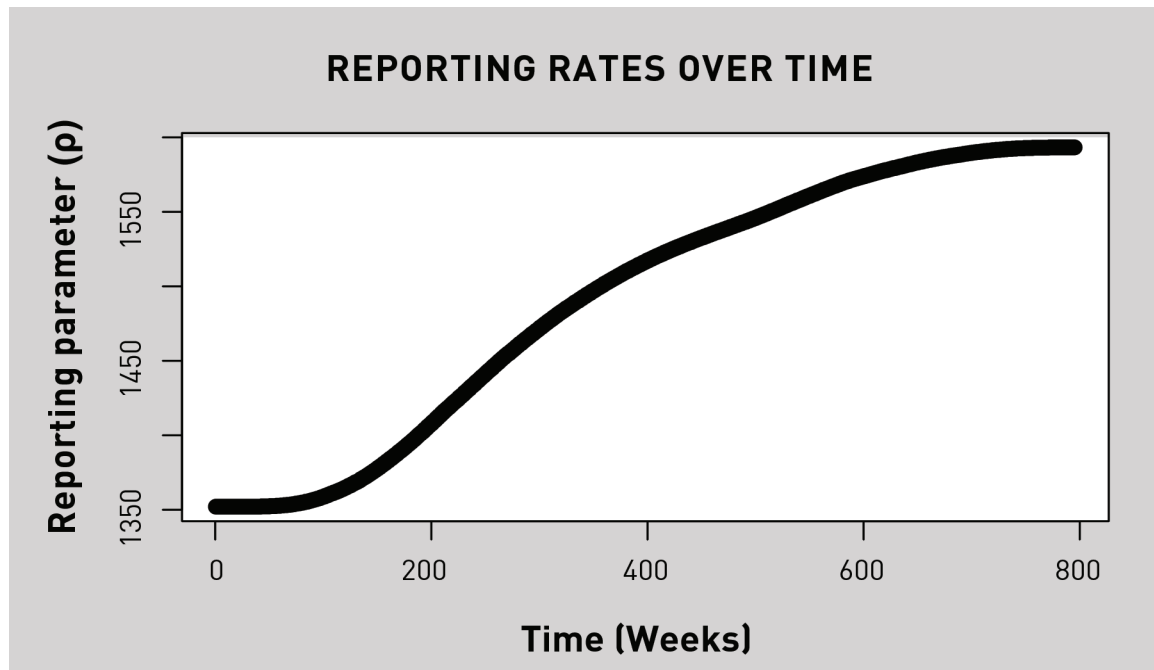


FIGURE A3: DERIVATION OF MEAN SUSCEPTIBLES. The mean susceptible value was derived as the minimum of the deviance of the regression, here termed “log likelihood.”

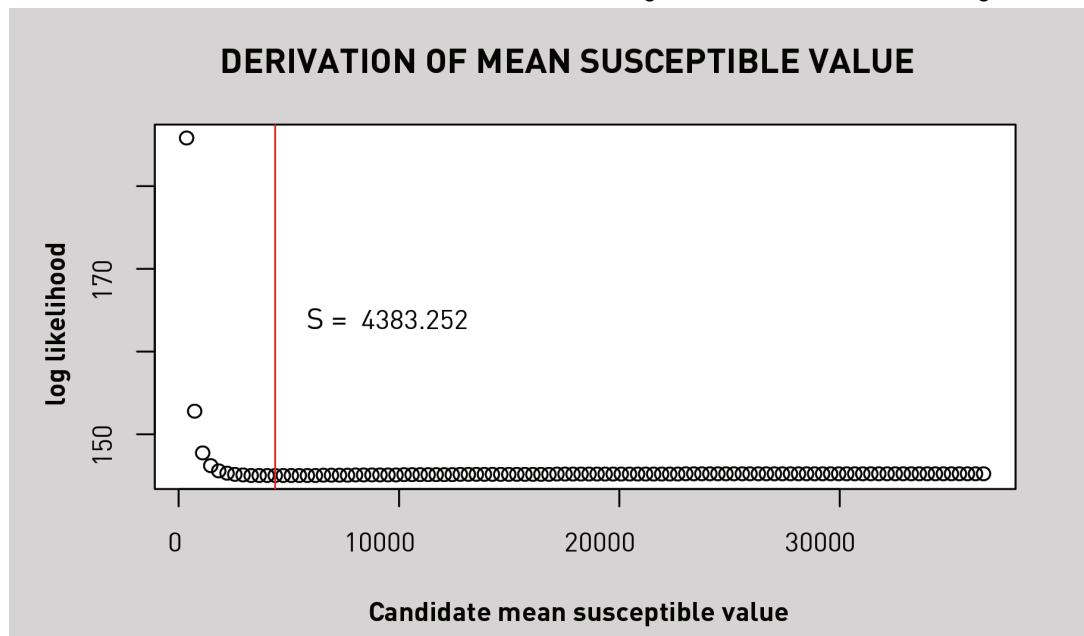


FIGURE A4: REGRESSION OF FOOD AGAINST LOVE. Food is found to equal love.

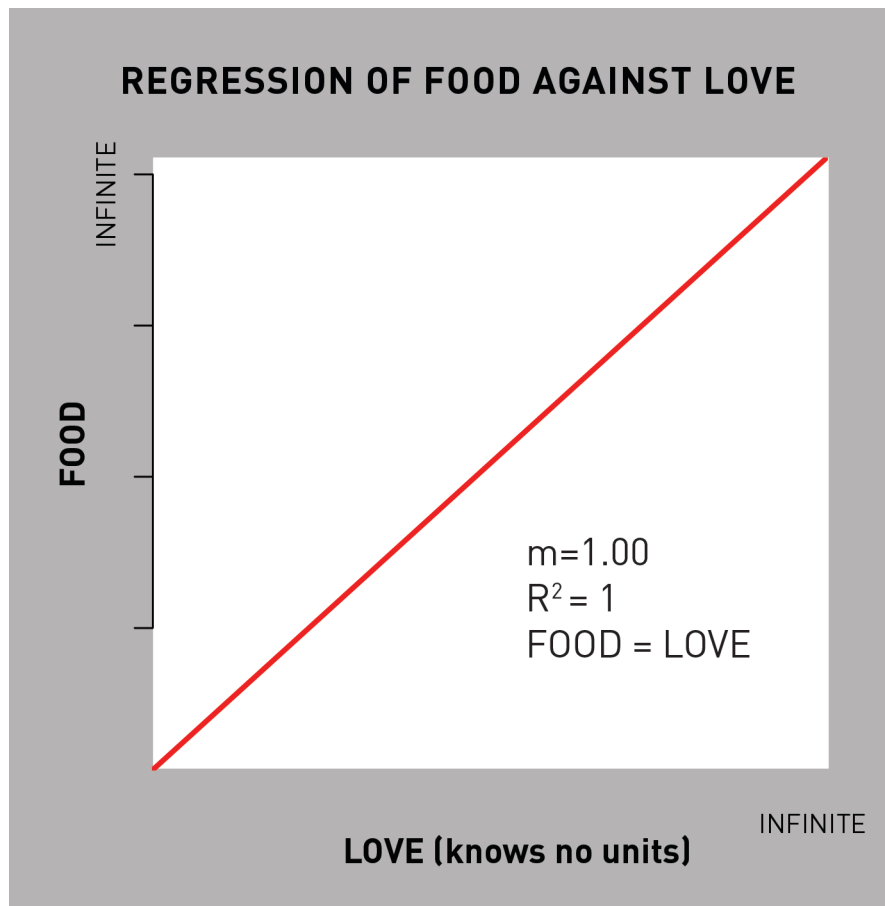


TABLE 1: TRANSMISSION PARAMETER (β) ESTIMATION RESULTS

Week	<i>log value</i>	<i>Standard error</i>	<i>Actual value</i> ($\times 10^{-4}$)
1	-7.0360229	0.19261	8.796180
2	-7.0971697	0.19382	8.274435
3	-7.0974080	0.19382	8.272464
4	-7.2589904	0.19383	7.038182
5	-7.1443114	0.19117	7.893416
6	-7.1749010	0.19086	7.655615
7	-7.0443964	0.19011	8.722832
8	-7.1948064	0.19163	7.504734
9	-7.1342410	0.19043	7.973307
10	-6.9348674	0.19043	9.732521
11	-7.1011744	0.19372	8.241365
12	-7.0081619	0.19372	9.044696
13	-7.1399888	0.19527	7.927609
14	-6.9512704	0.19438	9.574180
15	-7.1539309	0.19677	7.817849
16	-6.6447938	0.19540	13.007766
17	-6.9200020	0.20278	9.878279
18	-7.1282434	0.20432	8.021272
19	-7.0094575	0.20208	9.032985
20	-6.8739301	0.20221	10.344038
21	-6.9747177	0.20462	9.352303
22	-6.9930452	0.20490	9.182460
23	-6.9059193	0.20481	10.018377
24	-7.0930944	0.20620	8.308225
25	-7.0638885	0.20417	8.554452
26	-6.9237174	0.20296	9.841646
27	-7.1598819	0.20432	7.771463
28	-7.0683289	0.20144	8.516551
29	-7.1561050	0.20060	7.800870
30	-7.0112121	0.19843	9.017149
31	-7.0480158	0.19906	8.691318
32	-7.1679977	0.19896	7.708647
33	-7.0029845	0.19688	9.091645
34	-7.0943499	0.19790	8.297800
35	-7.3259770	0.19723	6.582162
36	-6.8447707	0.19283	10.650104
37	-7.1528632	0.19716	7.826201
38	-7.1022974	0.19564	8.232115
39	-6.9418232	0.19523	9.665058
40	-7.1332619	0.19756	7.981118
41	-6.9871398	0.19631	9.236847
42	-7.1728658	0.19770	7.671212

43	-7.0657553	0.19577	8.538498
44	-7.0250371	0.19594	8.893346
45	-7.1324958	0.19677	7.987234
46	-7.0294801	0.19567	8.853920
47	-7.2069253	0.19648	7.414334
48	-7.1018746	0.19420	8.235597
49	-7.1137220	0.19405	8.138602
50	-7.0979857	0.19374	8.267686
51	-7.0981823	0.19374	8.266061
52	-7.1716684	0.19375	7.680402
53	-7.0913231	0.19518	8.322954

References

- [1] L. Chang, K. Tsao, S. Hsia, and S. Shih, “Transmission and clinical features of enterovirus 71 infections in household contacts in Taiwan,” *Jama*, vol. 291, no. 2, 2004.
- [2] P. McMinn, “An overview of the evolution of enterovirus 71 and its clinical and public health significance,” *FEMS Microbiol. Rev.*, vol. 26, 2002.
- [3] T.-Y. Lin, S.-J. Twu, M.-S. Ho, L.-Y. Chang, and C.-Y. Lee, “Enterovirus 71 outbreaks, Taiwan: occurrence and recognition.,” *Emerg. Infect. Dis.*, vol. 9, no. 3, pp. 291–3, Mar. 2003.
- [4] M. Ho, E. Chen, and K. Hsu, “An epidemic of enterovirus 71 infection in Taiwan,” ... *Engl. J. ...*, vol. 341, no. 13, pp. 929–935, 1999.
- [5] D. Zhang, J. Lu, and J. Lu, “Enterovirus 71 vaccine: close but still far.,” *Int. J. Infect. Dis.*, vol. 14, no. 9, pp. e739–43, Sep. 2010.
- [6] G. Nagy, S. Tak□tsy, E. Kuk□n, I. Mih□ly, and I. D□m□k, “Virological diagnosis of enterovirus type 71 infections: Experiences gained during an epidemic of acute CNS diseases in Hungary in 1978,” *Arch. Virol.*, vol. 71, no. 3, pp. 217–227, Sep. 1982.
- [7] G. L. Gilbert, K. E. Dickson, M. J. Waters, M. L. Kennett, S. A. Land, and M. Sneddon, “Outbreak of enterovirus 71 infection in Victoria, Australia, with a high incidence of neurologic involvement.,” *Pediatr. Infect. Dis. J.*, vol. 7, no. 7, pp. 484–8, Jul. 1988.
- [8] E. Ma, T. Lam, K. C. Chan, C. Wong, and S. K. Chuang, “Changing epidemiology of hand, foot, and mouth disease in Hong Kong, 2001-2009.,” *Jpn. J. Infect. Dis.*, vol. 63, no. 6, pp. 422–6, Nov. 2010.
- [9] Y. Ishimaru, S. Nakano, K. Yamaoka, and S. Takami, “Outbreaks of hand, foot, and mouth disease by enterovirus 71. High incidence of complication disorders of central nervous system.,” *Arch. Dis. Child.*, vol. 55, no. 8, pp. 583–8, Aug. 1980.
- [10] S. Singh, V. T. K. Chow, M. C. Phoon, K. P. Chan, and C. L. Poh, “Direct Detection of Enterovirus 71 (EV71) in Clinical Specimens from a Hand, Foot, and Mouth Disease Outbreak in Singapore by Reverse Transcription-PCR with Universal Enterovirus and EV71-Specific Primers,” *J. Clin. Microbiol.*, vol. 40, no. 8, pp. 2823–2827, Aug. 2002.
- [11] S. AbuBakar, H.-Y. Chee, M. F. Al-Kobaisi, J. Xiaoshan, K. Bing Chua, and S. Kit Lam, “Identification of enterovirus 71 isolates from an outbreak of HFMD with fatal cases of encephalomyelitis in Malaysia,” *Virus Res.*, vol. 61, no. 1, pp. 1–9, May 1999.

- [12] N.-Z. Ding, X.-M. Wang, S.-W. Sun, Q. Song, S.-N. Li, and C.-Q. He, “Appearance of mosaic enterovirus 71 in the 2008 outbreak of China.,” *Virus Res.*, vol. 145, no. 1, pp. 157–61, Oct. 2009.
- [13] J. Xu, Y. Qian, S. Wang, J. M. G. Serrano, W. Li, Z. Huang, and S. Lu, “EV71: an emerging infectious disease vaccine target in the Far East?,” *Vaccine*, vol. 28, no. 20, pp. 3516–21, Apr. 2010.
- [14] S.-C. Chu, E.-T. Wang, and D.-P. Liu, “Is a monovalent vaccine against enterovirus 71 sufficient? A review of enterovirus 71 vaccine development based on enterovirus surveillance in Taiwan.,” *J. Formos. Med. Assoc.*, vol. 112, no. 9, pp. 508–9, Sep. 2013.
- [15] E. Tseng, “Project Proposal : Modeling the Spread of Enterovirus-71 in Taiwan,” 2013.
- [16] K. K. Tee, T. T. Lam, Y. F. Chan, J. M. Bible, A. Kamarulzaman, C. Y. W. Tong, Y. Takebe, and O. G. Pybus, “Evolutionary genetics of human enterovirus 71: origin, population dynamics, natural selection, and seasonal periodicity of the VP1 gene.,” *J. Virol.*, vol. 84, no. 7, pp. 3339–50, Apr. 2010.
- [17] X. Chen, Q. Zhang, J. Li, W. Cao, J.-X. Zhang, L. Zhang, W. Zhang, Z.-J. Shao, and Y. Yan, “Analysis of recombination and natural selection in human enterovirus 71.,” *Virology*, vol. 398, no. 2, pp. 251–61, Mar. 2010.
- [18] P. Plevka, R. Perera, J. Cardosa, R. J. Kuhn, and M. G. Rossmann, “Crystal structure of human enterovirus 71.,” *Science*, vol. 336, no. 6086, p. 1274, Jun. 2012.
- [19] B. a Brown, M. S. Oberste, J. P. Alexander, M. L. Kennett, and M. a Pallansch, “Molecular epidemiology and evolution of enterovirus 71 strains isolated from 1970 to 1998.,” *J. Virol.*, vol. 73, no. 12, pp. 9969–75, Dec. 1999.
- [20] K. Mizuta, C. Abiko, T. Murata, Y. Matsuzaki, T. Itagaki, K. Sanjoh, M. Sakamoto, S. Hongo, S. Murayama, and K. Hayasaka, “Frequent Importation of Enterovirus 71 from Surrounding Countries into the Local Community of Yamagata, Japan, between 1998 and 2003,” vol. 43, no. 12, pp. 6171–6175, 2005.
- [21] K. Mizuta, Y. Aoki, A. Suto, K. Ootani, N. Katsushima, T. Itagaki, A. Ohmi, M. Okamoto, H. Nishimura, Y. Matsuzaki, S. Hongo, K. Sugawara, H. Shimizu, and T. Ahiko, “Cross-antigenicity among EV71 strains from different genogroups isolated in Yamagata, Japan, between 1990 and 2007.,” *Vaccine*, vol. 27, no. 24, pp. 3153–8, May 2009.
- [22] E. C. McWilliam Leitch, M. Cabrerizo, J. Cardosa, H. Harvala, O. E. Ivanova, S. Koike, a C. M. Kroes, a Lukashev, D. Perera, M. Roivainen, P. Susi, G. Trallero, D. J. Evans, and P. Simmonds, “The association of recombination events in the founding and emergence of subgenogroup evolutionary lineages of human enterovirus 71.,” *J. Virol.*, vol. 86, no. 5, pp. 2676–85, Mar. 2012.

- [23] E. Tseng, “Rapid Molecular Adaptive Evolution of EV-71: Consequences for Vaccine Development,” 2013.
- [24] N. J. Schmidt, E. H. Lennette, and H. H. Ho, “An apparently new enterovirus isolated from patients with disease of the central nervous system.,” *J. Infect. Dis.*, vol. 129, no. 3, pp. 304–9, Mar. 1974.
- [25] J. Bible and P. Pantelidis, “Genetic evolution of enterovirus 71: epidemiological and pathological implications,” *Rev. Med.* ..., no. May, pp. 371–379, 2007.
- [26] M. Chumakov, M. Voroshilova, L. Shindarov, I. Lavrova, L. Gracheva, G. Koroleva, S. Vasilenko, I. Brodvarova, M. Nikolova, S. Gyurova, M. Gacheva, G. Mitov, N. Ninov, E. Tsylka, I. Robinson, M. Frolova, V. Bashkirtsev, L. Martiyanova, and V. Rodin, “Enterovirus 71 isolated from cases of epidemic poliomyelitis-like disease in Bulgaria.,” *Arch. Virol.*, vol. 60, no. 3–4, pp. 329–40, Jan. 1979.
- [27] L. M. Shindarov, M. P. Chumakov, M. K. Voroshilova, S. Bojinov, S. M. Vasilenko, I. Iordanov, I. D. Kirov, E. Kamenov, E. V Leshchinskaya, G. Mitov, I. A. Robinson, S. Sivchev, and S. Staikov, “Epidemiological, clinical, and pathomorphological characteristics of epidemic poliomyelitis-like disease caused by enterovirus 71.,” *J. Hyg. Epidemiol. Microbiol. Immunol.*, vol. 23, no. 3, pp. 284–95, Jan. 1979.
- [28] J. Blomberg, E. Lycke, K. Ahlfors, T. Johnsson, S. Wolontis, and G. von Zeipel, “Letter: New enterovirus type associated with epidemic of aseptic meningitis and/or hand, foot, and mouth disease.,” *Lancet*, vol. 2, no. 7872, p. 112, Jul. 1974.
- [29] Z.-M. Zheng, P.-J. He, D. Caufield, M. Neumann, S. Specter, C. C. Baker, and M. J. Bankowski, “Enterovirus 71 isolated from China is serologically similar to the prototype E71 BrCr strain but differs in the 5'-noncoding region,” *J. Med. Virol.*, vol. 47, no. 2, pp. 161–167, Oct. 1995.
- [30] K. T. Goh, S. Doraisingham, J. L. Tan, G. N. Lim, and S. E. Chew, “An outbreak of hand, foot, and mouth disease in Singapore.,” *Bull. World Health Organ.*, vol. 60, no. 6, pp. 965–9, Jan. 1982.
- [31] M. J. Cardosa, S. Krishnan, P. H. Tio, D. Perera, and S. C. Wong, “Isolation of subgenus B adenovirus during a fatal outbreak of enterovirus 71-associated hand, foot, and mouth disease in Sibu, Sarawak.,” *Lancet*, vol. 354, no. 9183, pp. 987–91, Sep. 1999.
- [32] M. Ho, “Enterovirus 71: the virus, its infections and outbreaks.,” *J. Microbiol. Immunol. Infect.*, vol. 33, no. 4, pp. 205–16, Dec. 2000.
- [33] L.-Y. Chang, C.-C. King, K.-H. Hsu, H.-C. Ning, K.-C. Tsao, C.-C. Li, Y.-C. Huang, S.-R. Shih, S.-T. Chiou, P.-Y. Chen, H.-J. Chang, and T.-Y. Lin, “Risk Factors of Enterovirus 71 Infection and Associated Hand, Foot, and Mouth Disease/Herpangina in Children During an Epidemic in Taiwan,” *Pediatrics*, vol. 109, no. 6, pp. e88–e88, Jun. 2002.

- [34] T.-Y. Lin, L.-Y. Chang, S.-H. Hsia, Y.-C. Huang, C.-H. Chiu, C. Hsueh, S.-R. Shih, C.-C. Liu, and M.-H. Wu, “The 1998 enterovirus 71 outbreak in Taiwan: pathogenesis and management.,” *Clin. Infect. Dis.*, vol. 34 Suppl 2, no. Suppl 2, pp. S52–7, May 2002.
- [35] Y. Chen, C. Li, D. He, T. Cheng, S. Ge, J. W.-K. Shih, Q. Zhao, P.-J. Chen, J. Zhang, and N. Xia, “Antigenic analysis of divergent genotypes human Enterovirus 71 viruses by a panel of neutralizing monoclonal antibodies: current genotyping of EV71 does not reflect their antigenicity.,” *Vaccine*, vol. 31, no. 2, pp. 425–30, Jan. 2013.
- [36] J. J. Yan, I. J. Su, P. F. Chen, C. C. Liu, C. K. Yu, and J. R. Wang, “Complete genome analysis of enterovirus 71 isolated from an outbreak in Taiwan and rapid identification of enterovirus 71 and coxsackievirus A16 by RT-PCR,” *J. Med.* ..., vol. 339, no. September 2000, pp. 331–339, Oct. 2001.
- [37] S.-P. Chen, Y.-C. Huang, W.-C. Li, C.-H. Chiu, C.-G. Huang, K.-C. Tsao, and T.-Y. Lin, “Comparison of clinical features between coxsackievirus A2 and enterovirus 71 during the enterovirus outbreak in Taiwan, 2008: a children’s hospital experience.,” *J. Microbiol. Immunol. Infect.*, vol. 43, no. 2, pp. 99–104, Apr. 2010.
- [38] Y. Chan and S. AbuBakar, “Recombinant Human Enterovirus 71 in Hand, Foot and Mouth Disease Patients,” *Emerg. Infect. Dis.*, vol. 10, no. 8, pp. 71–73, 2004.
- [39] N. C. Grassly, “The final stages of the global eradication of poliomyelitis.,” *Philos. Trans. R. Soc. Lond. B. Biol. Sci.*, vol. 368, no. 1623, p. 20120140, Aug. 2013.
- [40] F. C. S. Tiing, J. Labadin, F. Chuo, and S. T. S. Tiing, “A Simple Deterministic Model for the Spread of Hand, Foot and Mouth Disease (HFMD) in Sarawak,” *2008 Second Asia Int. Conf. Model. & Simul.*, pp. 947–952, May 2008.
- [41] N. Roy and N. Halder, “Compartmental modeling of hand, foot and mouth infectious disease (HFMD),” *Res. J. Appl. Sci.*, vol. 5, no. 3, pp. 177–182, 2010.
- [42] Y. Wang and F. Sung, “Modeling the infections for enteroviruses in Taiwan,” *Inst. Environ. Heal. China Med.* ..., pp. 1–23, 2004.
- [43] F.-C. Tseng, H.-C. Huang, C. Chi, T.-L. Lin, C.-C. Liu, J.-W. Jian, L.-C. Hsu, H.-S. Wu, J.-Y. Yang, Y. Chang, H. Wang, Y. Hsu, I.-J. Su, and J.-R. Wang, “Epidemiological survey of enterovirus infections occurring in Taiwan between 2000 and 2005: analysis of sentinel physician surveillance data.,” *J. Med. Virol.*, vol. 79, no. 12, pp. 1850–60, Dec. 2007.
- [44] M. Roberts and H. Heesterbeek, “Bluff your way in epidemic models,” *Trends Microbiol.*, vol. 1, no. 9, pp. 343–348, 1993.
- [45] R. Anderson, R. May, and B. Anderson, *Infectious Diseases of Humans: Dynamics and Control*. 1992.

- [46] P. Rohani, M. J. Keeling, and B. T. Grenfell, “The interplay between determinism and stochasticity in childhood diseases.,” *Am. Nat.*, vol. 159, no. 5, pp. 469–81, May 2002.
- [47] B. F. Finkenstädt and B. T. Grenfell, “Time series modelling of childhood diseases: a dynamical systems approach,” *J. R. Stat. Soc. Ser. C (Applied Stat.)*, vol. 49, no. 2, pp. 187–205, 2000.
- [48] O. BJØRNSTAD, “DYNAMICS OF MEASLES EPIDEMICS : ESTIMATING SCALING OF transmission rates using a time series SIR model,” *Ecol. ...*, vol. 72, no. 2, pp. 169–184, 2002.
- [49] O. Bjørnstad, “Dynamic models with environmental drivers,” pp. 1–22, 2007.
- [50] R. Breban, R. Vardavas, and S. Blower, “Theory versus data: how to calculate R_0 ?,” *PLoS One*, vol. 2, no. 3, p. e282, Jan. 2007.
- [51] K. Dietz, “The estimation of the basic reproduction number for infectious diseases,” *Stat. Methods Med. Res.*, vol. 2, no. 1, pp. 23–41, Mar. 1993.
- [52] S. Altizer, A. Dobson, P. Hosseini, P. Hudson, M. Pascual, and P. Rohani, “Seasonality and the dynamics of infectious diseases.,” *Ecol. Lett.*, vol. 9, no. 4, pp. 467–84, Apr. 2006.
- [53] C. J. E. Metcalf, O. N. Bjørnstad, B. T. Grenfell, and V. Andreasen, “Seasonality and comparative dynamics of six childhood infections in pre-vaccination Copenhagen.,” *Proc. Biol. Sci.*, vol. 276, no. 1676, pp. 4111–8, Dec. 2009.
- [54] B. T. Grenfell, O. N. Bjørnstad, and J. Kappey, “Travelling waves and spatial hierarchies in measles epidemics.,” *Nature*, vol. 414, no. 6865, pp. 716–23, Dec. 2001.
- [55] T.-C. Chan, J.-S. Hwang, R.-H. Chen, C.-C. King, and P.-H. Chiang, “Spatio-temporal analysis on enterovirus cases through integrated surveillance in Taiwan.,” *BMC Public Health*, vol. 14, p. 11, Jan. 2014.
- [56] W.-C. Huang, L. Huang, C.-L. Kao, C.-Y. Lu, P.-L. Shao, A.-L. Cheng, T.-Y. Fan, H. Chi, and L. Chang, “Seroprevalence of enterovirus 71 and no evidence of crossprotection of enterovirus 71 antibody against the other enteroviruses in kindergarten children in Taipei city.,” *J. Microbiol. Immunol. Infect.*, vol. 45, no. 2, pp. 96–101, Apr. 2012.
- [57] R. J. Duintjer Tebbens, M. A. Pallansch, J.-H. Kim, C. C. Burns, O. M. Kew, M. S. Oberste, O. M. Diop, S. G. F. Wassilak, S. L. Cochi, and K. M. Thompson, “Oral poliovirus vaccine evolution and insights relevant to modeling the risks of circulating vaccine-derived polioviruses (cVDPVs).,” *Risk Anal.*, vol. 33, no. 4, pp. 680–702, Apr. 2013.

- [58] J. O. Lloyd-Smith, S. J. Schreiber, P. E. Kopp, and W. M. Getz, “Superspreading and the effect of individual variation on disease emergence.,” *Nature*, vol. 438, no. 7066, pp. 355–9, Nov. 2005.

This thesis represents my own work in accordance with University regulations.